Journal of Materials Chemistry A

REVIEW

View Article Online
View Journal | View Issue



Cite this: J. Mater. Chem. A, 2021, 9, 20985

# Pyrolysis-free covalent organic framework-based materials for efficient oxygen electrocatalysis

Xun Cui, †*[ac] Likun Gao, †[bc] Rui Ma,[a] Zhengnan Wei,[d] Cheng-Hsin Lu,[ce] Zili Li [c] and Yingkui Yang *[a]

Received 2nd April 2021
Accepted 27th August 2021

DOI: 10.1039/d1ta02795f

rsc.li/materials-a

Low-cost and high-performance electrocatalysts towards oxygen electrocatalysis play a vital role in the widespread application of oxygen-based sustainable-energy technologies such as fuel cells, metal–air batteries and water electrolysis. Even though an enormous number of noble metal-free carbon-based materials have been proved to have comparable electrocatalytic performance to the noble metal-containing benchmarks, the unpredictable and poorly defined active sites resulting from the commonly required pyrolysis greatly hindered the insightful understanding of structure–activity relationships. Pyrolysis-free covalent organic frameworks (COFs) as a unique class of crystalline porous polymers provide an ideal platform for electrocatalysis research due to their tunable porosity, atomically precise structures and programmable topological architectures. Particularly, the elimination of high-temperature pyrolysis enables well-preserved active sites to gain deep insights into the electrocatalytic mechanisms. In this review, we first discuss the pros and cons of pyrolysis-free COFs for oxygen electrocatalysis. Then, recent advances in pyrolysis-free COF-based oxygen electrocatalysts are comprehensively

[a]Key Laboratory of Catalysis and Energy Materials Chemistry of Ministry of Education & Hubei Key Laboratory of Catalysis and Materials Science, South-Central University for Nationalities, Wuhan 430074, China. E-mail: xcui@scuec.edu.cn; ykyang@mail.scuec.edu.cn

[b]Key Laboratory of Bio-based Material Science and Technology of Ministry of Education, Northeast Forestry University, Harbin 150040, China

[c]School of Materials Science and Engineering, Georgia Institute of Technology, Atlanta, GA 30332, USA

[d]New Energy Development Centre, Shengli Petroleum Administration Co., Ltd, SINOPEC, China

[e]Instrumentation Center, National Tsing Hua University, Hsinchu 300044, Taiwan, China

† These authors contributed equally.

*Dr Xun Cui received his PhD degree in Chemical Engineering and Technology from Chongqing University, China, in 2018. He joined Prof Zhiqun Lin's group at the Georgia Institute of Technology, USA, as a visiting PhD student (2015–2017), where his research focused on the plasmonic enhancement of perovskite solar cells. After being a postdoctoral research fellow at the Georgia Institute of Technology, USA (2018–2020), he joined South-Central University for Nationalities, China, in 2020, and started his independent research mainly focusing on nanoscale surface science and materials engineering for electrocatalysis and electrochemical energy storage and conversion. He was recognized by the editors as an Outstanding Reviewer for the Journal of Materials Chemistry A in 2019.*

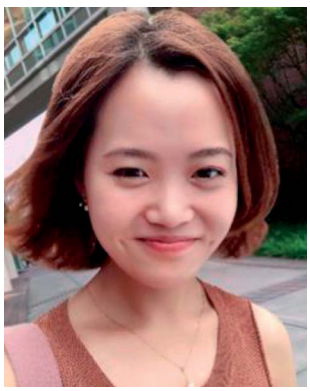

*Dr Likun Gao is currently a professor in the School of Material Science and Engineering at Northeast Forestry University, China. She received her PhD degree from the School of Materials Science and Engineering, Northeast Forestry University, China, in 2020. She worked as a visiting PhD student in Prof Zhiqun Lin's group in the School of Materials Science and Engineering at the Georgia Institute of Technology from 2018 to 2020. Her research interests mainly focus on the synthesis of novel wood-based functional materials and their applications in energy storage, electrocatalysis and photocatalysis.*

overviewed. The engineering strategies for pyrolysis-free COF-based oxygen electrocatalysts are discussed and paid particular attention, emphasizing their impact on electronic structure modulation and synergistic enhancement effect. Lastly, we also propose the key challenges and future perspectives for maximizing the superiorities of pyrolysis-free COF-based oxygen electrocatalysts. This article aims to emphasize the significance of pyrolysis-free COFs and their potential capability to outperform state-of-the-art noble metal-based electrocatalysts and promote the insightful understanding of structure–activity relationships.

## 1. Introduction

Clean and sustainable oxygen-based electrochemical energy conversion and generation technologies, such as fuel cells, metal–air batteries and water electrolysis, play an increasingly critical role in tackling the ever-growing demand for clean energy, rising global warming caused by $CO_2$ emissions, and environmental pollution issues worldwide.[1–5] As the most important electrode process in the practical operation of these sustainable energy technologies, oxygen electrocatalysis (*i.e.*, the oxygen reduction reaction (ORR) and oxygen evolution reaction (OER)) has always been the research hotspot of scientists in the past few decades due to the complicated reaction mechanisms and sluggish reaction kinetics.[6–8] Fundamentally, the electrocatalytic ORR process is a complex multi-electron transfer electrochemical reaction and generally proceeds either *via* a two-electron ($2e^-$) pathway with the production of $H_2O_2$ (acidic conditions) or $HO_2^-$ (alkaline or neutral conditions) as the oxygenated intermediate or through a more efficient four-electron ($4e^-$) pathway to directly convert $O_2$ into $H_2O$ (acidic conditions) or $OH^-$ (alkaline or neutral conditions) (Table 1).[9,10] The OER process is also very complicated as it is intrinsically the reverse version of the ORR and generally involves a concerted four-electron–proton transfer to yield $O_2$, as described in Table 1.[11] Although platinum (Pt)-based materials and ruthenium/iridium-based oxides ($RuO_2$/$IrO_2$) have been long recognised as the state-of-the-art ORR and OER electrocatalysts, respectively, their inherent drawbacks of prohibitive cost, small reserve and poor stability have greatly

*Rui Ma received his B.S. in Applied Chemistry from South-Central University for Nationalities in 2020. He is currently pursuing his M.S. in Physical Chemistry at South-Central University for Nationalities. His research interests focus on the design and synthesis of functional polymers for electrochemical energy storage and conversion.*

*Dr Cheng-Hsin (Johnson) Lu obtained his Master's and PhD degrees in Materials Science and Engineering from the University of Pennsylvania in 2010 and Drexel University in 2016, respectively. He then joined Prof Zhiqun Lin's group in the School of Materials Science and Engineering at the Georgia Institute of Technology to work as a postdoctoral research associate. His work involves the synthesis and characterization of semiconductor nanoparticles, including traditional II–VI and IV–VI semiconductor quantum dots, novel all-inorganic and organic–inorganic hybrid metal halide perovskite nanocrystals, and their optoelectronic applications.*

*Dr Zhengnan Wei received his PhD degree in Chemical Engineering and Technology from Chongqing University, China, in 2018. He then joined the Postdoctoral Scientific Research Station of Shengli Petroleum Administration, SINOPEC, China, in 2019, to work as a postdoctoral research associate. His primary domain of research is electrochemical energy conversion and green energy development and utilization.*

*Dr Yingkui Yang is currently a professor in the School of Chemistry and Materials Science at South-Central University for Nationalities. He received his PhD degree in Polymer Chemistry and Physics from Huazhong University of Science and Technology in 2007. His current research focuses on advanced polymers for energy conversion and storage, graphene industrialization and electronic functional materials.*

 

Table 1 Oxygen electrocatalysis in acid, neutral and alkaline media, respectively (the symbol "*" represents the active site that absorbs reactants, intermediates, and products)

| Oxygen reduction reaction (ORR) | Oxygen evolution reaction (OER) |
|---|---|
| **Acid media**<br>$O_2 + 4H^+ + 4e^- \rightarrow 2H_2O$ ($4e^-$ pathway: $O_2 + H^+ + e^- \rightarrow OOH^*$; $OOH^* + H^+ + e^- \rightarrow O^* + H_2O$; $O^* + H^+ + e^- \rightarrow OH^*$; $OH^* + H^+ + e^- \rightarrow H_2O$) or ($2e^-$ pathway: $O_2 + 2H^+ + 2e^- \rightarrow H_2O_2^*$; $H_2O_2^* + 2H^+ + 2e^- \rightarrow 2H_2O$) | **Acid or neutral media**<br>$2H_2O \rightarrow O_2 + 4H^+ + 4e^-$ ($H_2O \rightarrow OH^* + H^+ + e^-$; $OH^* \rightarrow O^* + H^+ + e^-$; $O^* + O^* \rightarrow O_2$ or $O^* + H_2O \rightarrow OOH^* + H^+ + e^-$; $OOH^* \rightarrow O_2 + H^+ + e^-$) |
| **Neutral or alkaline media**<br>$O_2 + 2H_2O + 4e^- \rightarrow 4OH^-$ ($4e^-$ pathway: $O_2 + H_2O + e^- \rightarrow OOH^* + OH^-$; $OOH^* + e^- \rightarrow O^* + OH^-$; $O^* + H_2O + e^- \rightarrow OH^* + OH^-$; $OH^* + e^- \rightarrow OH^-$; or $2e^-$ pathway: $O_2 + H_2O + 2e^- \rightarrow HO_2^{-*} + OH^-$; $HO_2^{-*} + H_2O + 2e^- \rightarrow 3OH^-$) | **Alkaline media**<br>$4OH^- \rightarrow O_2 + 2H_2O + 4e^-$ ($OH^- \rightarrow OH^* + e^-$; $OH^* + OH^- \rightarrow O^* + H_2O + e^-$; $O^* + O^* \rightarrow O_2$ or $O^* + OH^- \rightarrow OOH^* + e^-$; $OOH^* + OH^- \rightarrow O_2 + H_2O + e^-$) |



hampered the large-scale commercial application of fuel cells, metal–air batteries and water electrolysis.[12–14] Accordingly, the development of cost-efficient noble metal-free oxygen electrocatalysts with improved activity and enhanced durability is crucial for the large-scale application of these sustainable electrochemical energy technologies.

The last few decades have witnessed continuous endeavour and enormous achievements in the development of low-cost and high-efficiency catalysts towards oxygen electrocatalysis.[15–19] Various noble metal-free electrocatalysts, particularly carbon-based materials, have been developed and proved to have comparable electrocatalytic performance to the noble metal-containing benchmarks.[20,21] Particularly, earth-abundant transition metal-containing carbonaceous materials have been considered as promising alternatives to the state-of-the-art noble metal-based oxygen electrocatalysts.[22,23] Nevertheless, the synthesis approaches for a majority of these carbon-based electrocatalysts generally require a high-temperature (usually 700–1100 °C) pyrolysis procedure of the precursor mixture to improve the electrical conductivity, electrocatalytic activity, and corrosion resistance, inevitably leading to undesirable structure changes and/or even reconstruction of the original fine structure.[24,25] Notably, the high-temperature pyrolysis treatment also results in the generation of unpredictable and poorly defined electrocatalytically active sites which brings great challenges to the structure–property relationships, severely hindering the insightful understanding of the reaction mechanisms.[26,27] To this end, the development of a pyrolysis-free strategy towards the synthesis of carbon-based electrocatalysts can certainly avoid the disadvantages mentioned above. Indeed, a pyrolysis-free strategy can simultaneously and efficiently reduce the energy consumption, improve the repeatability of material preparation, and realize the controllable construction of high-density, high-efficiency and well-defined active sites at the atomic level, providing model electrocatalysts for revealing the structure–activity relationships and electrocatalytic mechanisms.

Along with the massive advancement of porous organic polymers since Yaghi's group reported the pyrolysis-free covalent organic frameworks (COFs), various pyrolysis-free COF-based materials engineered to possess well-defined electrocatalytically active sites have shown superior potential in electrocatalysis due to their precisely controllable capacities regarding active site positioning and porosity/channel tailoring.[28–30] The pyrolysis-free COFs are generally formed *via* the polymerization of organic monomers under certain conditions and essentially a unique class of polymers as they integrate secondary structural organic units (*i.e.*, monomers) into a predictable long-range-ordered structure.[31–33] The periodic structure of pyrolysis-free COFs intrinsically consists of two main parts: one is the ordered framework and the other is the arrayed pores/channels. On the basis of these two unique characteristics, pyrolysis-free COFs offer a desirable platform for engineering pre-designed monomers to implement an anticipated skeleton and porosity/channel. On the other hand, the absence of high-temperature pyrolysis treatment during the synthesis of pyrolysis-free COF-based materials completely preserves the pre-designed active sites, therefore ensuring clear structure–activity relationships and thus offering an inherent superiority for electrocatalytic mechanism studies and performance optimization of the electrocatalysts.[34,35]

To manipulate the electrocatalytic activity of pyrolysis-free COF-based materials, the engineering strategies should be focused on the intrinsic activity of the active sites, number of exposed active sites, electronic conductivity, stability, and structural design. As described in Fig. 1, massive endeavours have been made to improve the performance of pyrolysis-free COF-based oxygen electrocatalysts. Fundamentally, the intrinsic activity of pyrolysis-free COF-based materials is determined by the electronic structure of active sites and thus can be manipulated *via* optimizing the electronic properties of active sites to tune the binding energy towards key reaction intermediates.[36–38] Indeed, heteroatoms and substituents are generally employed to modify the chemical environment of active sites. Besides, the reasonable construction of nanoarchitectures, such as diverse geometric configurations, rational pore size distribution, and appropriate crystalline degree, can maximize the exposed active sites and ensure rapid mass transport.[39–41] Furthermore, the electron transfer capability of electrocatalysts is also extremely crucial in electrochemical processes. In addition to building fully conjugated frame structures, many investigators have been focused on the combination of pyrolysis-free COFs with high-surface-area conductive supporting materials (*e.g.*, graphene, carbon nanotubes (CNTs) and

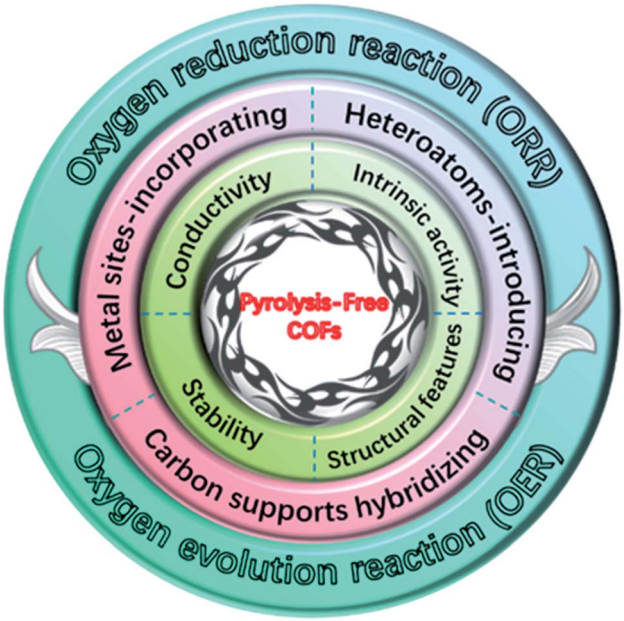


Fig. 1 Schematic diagram of the topics involved in this review.

carbon nanoparticles).[42–44] In fact, these conductive supports on the one hand can be used as templates to guide the growth of COFs and minimize the π–π stacking of COFs, and on the other hand can also serve as current collectors to simultaneously improve the electronic conductivity. The obtained pyrolysis-free COF/support hybridization has been proven to be a practical route for upgrading the activity of active sites caused by the enhanced electronic conductivity and synergistic effect between pyrolysis-free COFs and conductive supports.

In this review, we first discuss the pros and cons of pyrolysis-free COFs for oxygen electrocatalysis based on intrinsic activity, electrical conductivity, stability and structural features. Then, the recent developments of pyrolysis-free COF-based materials for oxygen electrocatalysis are comprehensively summarized. Particular attention is paid to engineering strategies to manipulate the electrocatalytic activity and the structure–activity correlations. At the end, future perspectives regarding the challenges and opportunities awaiting this research area are proposed and discussed. Although pyrolysis-free COF-based electrocatalysts are still in the infancy stage, they play an important role in promoting the study of electrocatalytic mechanisms. We hope that this review can offer some valuable references for future engineering of high-efficiency electrocatalysts with practical application capabilities.

## 2. Key factors for constructing efficient pyrolysis-free COF-based oxygen electrocatalysts

Since the performance of oxygen electrocatalysis is of course mainly determined by the electrocatalysts, it is critical to develop electrocatalysts with favourable catalytic activity, desired selectivity, and superior durability. Particularly, the exposed electrocatalytically active sites dominate the catalytic activity and selectivity, playing a pivotal role in reducing reaction energy barriers. Therefore, considerable attention has to be paid to the intrinsic activity of active sites and the density of exposed active sites as the electrocatalytic process only occurs on these exposed catalytically active sites. At the same time, considering that the oxygen electrocatalysis reactions involve multiple electrons and diverse oxygen-containing intermediates, certain electron-transfer and mass-transport pathways within the electrocatalysts for fast electron transfer and rapid mass transport are necessary for satisfactory electrocatalytic activities. In this section, we first give a brief overview of the pros and cons of pyrolysis-free COF-based materials when applied for oxygen electrocatalysis. Then, a detailed analysis of pyrolysis-free COF-based materials from the following four aspects: intrinsic activity, electrical conductivity, stability, and structural features, is provided.

### 2.1 The pros and cons of pyrolysis-free COFs for oxygen electrocatalysis

Pyrolysis-free COFs, as a subclass of porous polymers with rigid skeletons, periodic topological architectures and permanent porosity, are generally composed of molecular secondary building blocks strongly connected *via* covalent bonds. The flexibility in the selection of the secondary building blocks offers great possibilities to create a variety of accessible topological architectures with desired physicochemical properties in a precisely controllable manner. Accordingly, pyrolysis-free COFs possess some intriguing characteristics, such as ultra-large specific surface area (up to 4210 $m^2\ g^{-1}$), designable pore sizes (up to 4.7 nm), exceptional thermal stability (up to 600 °C), and high charge mobility (up to 8.1 $cm^2\ V^{-1}\ s^{-1}$).[29,45] Notably, as pyrolysis-free COFs are generally composed of earth-rich and inexpensive elements, pyrolysis-free COF-based materials will also possess an advantage in terms of price with the rapid development of synthesis technologies. These collective features make pyrolysis-free COF-based materials an interesting type of material and promising candidates for electrochemical applications.

Generally, pyrolysis-free COF-based materials have the following pros that are beneficial for oxygen electrocatalysis: (i) varieties of secondary building blocks and linkage motifs enable the construction of well-designed topological structures and functionalities; (ii) rich micro-/mesopores uniformly dispersed in the long-range ordered skeleton provide abundant space for loading a high density of well-defined active sites; (iii) the tuneable porosities (*i.e.*, pore sizes and pore geometries) contribute to the rational confinement of active moieties, such as single atoms, nanoclusters, and nanoparticles; (iv) the periodic topological architectures ensure the precise control of the electrocatalytically active sites, providing the possibility of understanding the structure–activity relationships; (v) the secondary building blocks that typically contain nitrogen-containing groups (*e.g.*, bipyridines, porphyrins, *etc.*) can serve as coordination sites for metal incorporation within the skeleton, resulting in atomically dispersed metal electrocatalysts;

 

(vi) the robust covalent interactions between the secondary building blocks endow pyrolysis-free COFs with high chemical stability and long-term durability under harsh electrochemical conditions and make the post-synthetic modification feasible. Based on these pros, much effort and some encouraging progress in the utilization of pyrolysis-free COF-based materials for oxygen electrocatalysis have been made. Up to now, various pyrolysis-free COF-based materials for efficient oxygen electrocatalysis have been demonstrated.

Nevertheless, despite the aforementioned pros, the following several cons of pyrolysis-free COF-based materials when applied for oxygen electrocatalysis have to be considered and addressed: (i) the pores present in the skeleton of pyrolysis-free COFs are mainly in the form of micropores and/or small mesopores, which inhibit mass transport and prevent access to the deep-buried abundant active sites during oxygen electrocatalysis; (ii) although pyrolysis-free COFs could theoretically be highly conductive as a result of the π-conjugation and overlapped π electron clouds, the reported charge carrier mobility is still lower than that of common inorganic electrocatalytic materials; (iii) the pyrolysis-free COFs are generally obtained in the form of bulk powder, in which the long channels formed by the densely stacked COF layers pose a great obstacle for mass transport and full utilization of active sites. To overcome these disadvantages, a sequence of pyrolysis-free COF-based materials with hierarchically porous structures and pyrolysis-free COF/conductive support hybrids have been proposed very recently, which consequently receive significant attention in this present review.

### 2.2 Intrinsic activity

The complete oxygen electrocatalysis in aqueous solutions is an extremely complicated multi-electron electrochemical process, which generally involves the adsorption and desorption of reactant molecules, diverse oxygen-containing intermediates and products on the active sites depending on the pH conditions of the electrolytes, as described in Table 1. Basically, oxygen-containing species are sequentially adsorbed on active sites during the electrocatalytic process. Accordingly, the reactivity of each step depends largely on the interaction between these corresponding oxygen-containing intermediates and the active sites. Therefore, the overall reaction energy barrier of oxygen electrocatalysis mainly stems from the adsorption and desorption of the above-mentioned intermediates (*i.e.*, O*, OH*, OOH*, *etc.*) during the reactions, which are closely related to the surface properties and essentially determine the overall reactivity of oxygen electrocatalysts. Specifically, too strong adsorption of the oxygen-containing species on the active sites will make the products difficult to desorb. In contrast, too weak interaction between the oxygen-containing species and the active sites will result in low probability of reactant adsorption. As a consequence, high-performance oxygen electrocatalysts require a moderate adsorption energy of the oxygen-containing intermediates. By rationally modulating the electronic structure of the active sites, the adsorption energies can reach suitable values, thus achieving optimal electrocatalytic activity.

In this context, the intrinsic activity of pyrolysis-free COF-based oxygen electrocatalysts depends greatly on the surface properties (*e.g.*, the exposed functional groups, the suspended bonds, the surface charge distribution, *etc.*). For instance, the exposed functional groups on the surface of pyrolysis-free COF-based electrocatalysts, such as the strongly electron-donating carbonyl groups, are capable of absorbing oxygen molecules, thereby enabling the electrocatalytic ORR process.[46] However, strongly electron-withdrawing functional groups such as the pyridinic-N groups favour the electrocatalytic OER process.[47] Consequently, the intrinsic activity of pyrolysis-free COF-based oxygen electrocatalysts can be significantly improved *via* the manipulation of the surface properties by tailoring the electronic structure and adjusting the chemical environment of the active sites, such as by introducing heteroatoms and incorporating non-noble metal-containing units, which will be discussed in detail in the following sections. In addition, the utilization efficiency of these highly intrinsically active sites should be considered to improve their accessibility to oxygen, electrolyte, and electrons. Accordingly, both intrinsic activity manipulation and structure design should be combined to promote the performance of pyrolysis-free COF-based oxygen electrocatalysts.

### 2.3 Electrical conductivity

In terms of electron transfer, the electrical conductivity of an electrocatalyst is vital to high-efficiency oxygen electrocatalysis. The active materials are expected to provide high electrical conductivity which can reduce electron transfer resistance, facilitate electron transfer and improve electrochemical polarization. In fact, conductivity is essentially the ability of a material to conduct electrical and thermal energy and dominated by the band structure, charge carrier concentration and their mobility.[48,49] Accordingly, organic polymers generally have relatively low electrical conductivity compared to traditional metal-based materials due to the absence of sufficient free electrons which can freely delocalize across the surface.

Since pyrolysis-free COFs are completely comprised of secondary organic building blocks bonded together by strong covalent interactions, most of the pyrolysis-free COFs possess π-conjugated structures and therefore show at least a modest electronic conductivity.[50] Furthermore, the π-conjugated structures ensure many pyrolysis-free COF semiconducting properties. As a result, the bandgap structure, carrier concentration and mobility (*i.e.* electrical conductivity) can be easily modulated by emulating conventional semiconductor engineering approaches, such as heteroatom incorporation, dopant control and chemical environment manipulation.[28] For example, the intrinsic electronic conductivity of pyrolysis-free COFs can be successfully leveraged by rational selection of aromatic building blocks to maximize the orbital overlap.[51,52] Moreover, the length of the π-conjugated chain which significantly influences the band gap also can be controlled to tune the electronic properties of pyrolysis-free COF-based materials.[53] Nonetheless, the electrical conductivity of pyrolysis-free COFs is still inferior to that of other typical inorganic electrocatalytic materials to date.

To this end, the construction of interfacial electron transfer channels *via* compositing pyrolysis-free COFs with highly conductive supporting materials, such as CNTs, graphene and carbon nanostructures, is another effective approach to circumvent the conductivity problem.

### 2.4 Stability

As to the oxygen electrocatalytic systems, electrochemical stability is also a basic requirement for active materials in the mutual conversion of electric energy and chemical energy. Generally, both the ORR and OER occur under severe electrochemical conditions, such as harsh acidic or basic conditions and high practical potentials. As a consequence, oxygen electrocatalysts should be designed to resist electrochemical corrosion over a long time.

Generally, high thermodynamic reversibility is usually required to attain exceptional crystallinity of pyrolysis-free COFs.[54] Therefore, some investigators doubt the chemical stability and electrochemical durability of pyrolysis-free COFs for practical oxygen electrocatalysis applications. In principle, the exclusive covalent connections can yield pyrolysis-free COFs with high chemical stability. To date, the ongoing developments have offered many pyrolysis-free COFs with stability under harsh acidic and/or basic conditions, and even some of them can tolerate strong oxidants and reductants without losing their porosity and crystallinity.[55,56] Covalent triazine frameworks (CTFs) have been recognized as some of the most stable pyrolysis-free COFs in strong acid and/or base media as well as strong oxidizing and reducing environments. Notably, most of the imine-, azine- and hydrazone-based pyrolysis-free COFs (connected by C=N bonds) possess superior stability under basic conditions. However, in acidic media, their stability still needs to be further improved because hydrolysis often occurs.[57] In this context, various approaches have also been proposed to effectively improve the stability of pyrolysis-free COFs, such as the post-modification of linkages to convert them into robust chemical bonds and the incorporation of particular functional groups to prevent hydrolysis.[54]

### 2.5 Structural features

In addition to the several aforementioned factors, the mass transport between the bulk phase and the surface of oxygen electrocatalysts is also an important factor that significantly influences the electrocatalytic performance.[58] In fact, both the ORR and OER involve gas (oxygen)/liquid (electrolyte) diffusion over the solid electrocatalyst surface and electron transfer between the active sites and current collector. As a consequence, the structural design of oxygen electrocatalysts has to be considered to enhance both the mass transport of oxygen/electrolyte and the electron transfer. In terms of mass transport, electrocatalysts with well-developed hierarchical porosity are highly desired, in which the macropores serve as the gas transport channels and the micropores and mesopores offer sufficient exposed active sites and reaction regions for gas/liquid/solid tri-phase electrocatalytic reactions. On the other hand, in addition to the highly expected high intrinsic electrical conductivity that can ensure fast electron transfer inside the electrocatalysts, a strong interaction between the electrocatalysts and current collectors is necessary to facilitate the electron transfer.

Pyrolysis-free COFs possess abundant micropores and/or small mesopores, which could guarantee the incorporation of high-density well-defined active sites. However, the lack of large mesopores and/or macropores undoubtedly impedes the mass transport of oxygen/electrolyte within the long channels and prevents access to the deep-buried abundant active sites during oxygen electrocatalysis, therefore leading to inferior electrocatalytic performance. Besides, the densely stacked COF layers of the generally obtained bulk pyrolysis-free COF powder also could result in poor mass transport and low utilization of active sites. In this regard, the design and construction of a-few-layer-thick pyrolysis-free COFs and hierarchically porous structured pyrolysis-free COFs are of particular interest for oxygen electrocatalysis. Notably, the combination of pyrolysis-free COFs with highly conductive substrates such as CNTs and graphene to form pyrolysis-free COF hybrids is promising not only to reduce the stacking of COF layers but also to offer abundant conducting channels to improve the electrical conductivity.

## 3. Metal-free pyrolysis-free COFs for oxygen electrocatalysis

### 3.1 The pivotal role of heteroatoms in oxygen electrocatalysis

For metal-free heteroatom-doped carbon-based materials including pyrolysis-free COFs, it has been well acknowledged that the intrinsic activity of active sites is closely connected with their local chemical environment which is basically determined by the difference in electronegativity between neighbouring atoms.[59–64] In comparison with the basic carbon atom, the most widely employed heteroatoms (*e.g.*, nitrogen (N), sulfur (S), boron (B), phosphorous (P), *etc.*) possess significantly different atomic size (in terms of van der Waals radius), electronegativity, valence electron number and electronic configuration, as comparatively summarized in Table 2.[65–69] Therefore, the incorporation of heteroatoms will cause distinct charge polarization and structural distortions, depending on the type and concentration of the incorporated heteroatom, resulting in the modification of the physical and chemical properties including charge density distribution, bandgap structure, chemical stability, and electronic conductivity. Notably, considering the diversity of these heteroatoms, the intrinsic activity of active sites can be accurately manipulated *via* charge density redistribution to provide high electrocatalytic activity and fulfill the requirements for oxygen electrocatalysis. Accordingly, the modulated electronic properties enable optimized binding energies of key oxygenated intermediates, hence improving the overall performance of oxygen electrocatalysis.

Particularly, pyrolysis-free COFs consist of periodically arranged monomers linked by covalent bonds in terms of structural composition. The incorporation of heteroatoms *via* reasonable monomer selection and precise manipulation at the

 

Table 2 Comparison of atomic size, electronegativity, valence electron number, and electronic configuration of different atoms

| Element | Nitrogen | Sulfur | Boron | Phosphorus | Carbon |
|---|---|---|---|---|---|
| Van der Waals radius (pm) | 155 | 180 | 180 | 195 | 170 |
| Electronegativity | 3.04 | 2.58 | 2.04 | 2.19 | 2.55 |
| Valence electron number | 5 | 6 | 3 | 5 | 4 |
| Electronic configuration | $1s^2 2s^2 2p^3$ | $1s^2 2s^2 2p^6 3s^2 3p^4$ | $1s^2 2s^2 2p^1$ | $1s^2 2s^2 2p^6 3s^2 3p^3$ | $1s^2 2s^2 2p^2$ |

atomic scale could undoubtedly ensure a long-range ordered arrangement of abundant heteroatoms, leading to well-defined active sites which are beneficial for the understanding of structure–activity relationships. In contrast, the common metal-free heteroatom-doped carbon-based materials obtained by conventional high-temperature pyrolysis possess a large number of poorly defined active sites, hindering the electrocatalytic mechanisms. Therefore, reasonable selection and introduction of heteroatoms are of great significance for pyrolysis-free COFs towards oxygen electrocatalysis.

Among these heteroatoms, the N atom is the most commonly adopted and widely investigated one in metal-free carbon-based materials including pyrolysis-free COFs for oxygen electrocatalysis. Generally, the electronegativity of the N atom (3.04) is significantly higher than that of the carbon atom (2.55) (Table 2).[70] With N-incorporation, the electroneutral carbon atoms will be perturbed due to the partial charge transfer from neighbouring carbon atoms to the N atom, causing an apparent positive polarization of the neighbouring carbon atom, thereby being favourable for both the electrocatalytic ORR and OER. When it comes to pyrolysis-free COFs, the similar atomic size of C and N as well as the diversity of N-containing monomers makes it extremely convenient to achieve N-incorporated pyrolysis-free COFs with considerable electrocatalytic activity. Moreover, although the S atom and P atom possess similar electronegativity (S: 2.58 and P: 2.19, respectively) compared with that of the carbon atom (2.55), their ability to enhance the electrocatalytic activity has also been verified. In fact, unlike N-incorporation, no visible charge transfer between the S (or P) atom and carbon atom can be detected after S or P-incorporation.[71,72] The function of the P atom is concluded to be the contribution of electrons to the oxygen molecule $2\pi^*$ states, leading to $O_2$ $2\pi^*$ state broadening and splitting and eventually enabling the stretching and weakening of the O–O bonds.[73,74] However, the electrocatalytic activity enhancement after S-incorporation can be attributed to the induced high charge delocalization and spin density of neighbouring carbon atoms.[75,76] The recently published literature has corroborated the promising potential of well-defined thiophene-S active site-containing pyrolysis-free COFs toward an effective electrocatalytic ORR.[77] In addition, the B atom with only one less valence electron compared to the neighbouring carbon atom has also been proven to be effective for the improvement of electrocatalytic ORR performance. Despite the lower electronegativity of the B atom (2.04) compared with that of the carbon atom (2.55), B-incorporation also induces charge polarization between the electron-donating B atoms and the neighbouring carbon atoms, leading to positively charged B atoms which are responsible for $O_2$ adsorption. Subsequently, the unoccupied $2p_z$ orbital of the B atom can accept $\pi$ electrons from the neighbouring carbon atom and then transfer them to the adsorbed $O_2$, effectively boosting the electrocatalytic ORR process.[78,79] Unfortunately, the common B-containing pyrolysis-free COFs (*e.g.*, boroxine- and boronate-ester-based COFs) are unstable in water as the electron-donating B sites are easily attacked by nucleophilic water molecules. Overall, the incorporation of heteroatoms with obvious difference in electronegativity compared with that of carbon atoms generally can deliver pyrolysis-free COFs with markedly improved electrocatalytic ORR activity mainly due to the induced positively charged active sites, while the heteroatoms with similar electronegativity may be more appropriate for the electrocatalytic OER.

### 3.2 Metal-free pyrolysis-free COFs for the electrocatalytic ORR

Based on the above discussion, the engineering of metal-free pyrolysis-free COFs *via* reasonable incorporation of heteroatoms will significantly modify their electronic properties, hence intrinsically constructing high-efficiency well-defined active sites. As a typical example of metal-free pyrolysis-free COF materials, covalent triazine frameworks (CTFs), which are composed of a periodic arrangement of interconnected 1,3,5-triazine structural units, have been demonstrated as effective pyrolysis-free COF-based electrocatalysts towards the ORR.[80] As exhibited in Fig. 2a–c, the presence of high concentration of N heteroatoms with relatively high electronegativity in the framework causes a distinct polarization of the whole system, so the electrons tend to accumulate on the N atoms, thereby resulting in the production of a large number of active sites and an appropriate bandgap structure to allow the electrocatalytic ORR process.[81] In addition, the robust C=N covalent bonds present in the triazine ring ensure excellent stability, and hence providing a good application prospect. Moreover, the polychlorotriphenylmethyl (PTM) radical based $\pi$-conjugated COF (PTM-CORF) with a small energy gap (*ca.* 0.88 eV) and a low-lying LUMO energy level (−4.72 eV) also displayed considerable electrocatalytic performance for the ORR.[82] The strongly electron-withdrawing characteristic of the PTM radical and the extended $\pi$-conjugation result in a half-wave potential ($E_{1/2}$) of 0.671 V (*vs.* RHE) and an electron transfer number of 3.89 under alkaline electrolyte conditions. In addition, a recently published study revealed that with the reasonable incorporation of S heteroatoms, highly efficient thiophene-S active sites for the ORR can be achieved. As can be seen in Fig. 2d, the as-prepared metal-free thiophene-sulfur covalent organic frameworks (MFTS-COFs), which comprise two different structural units

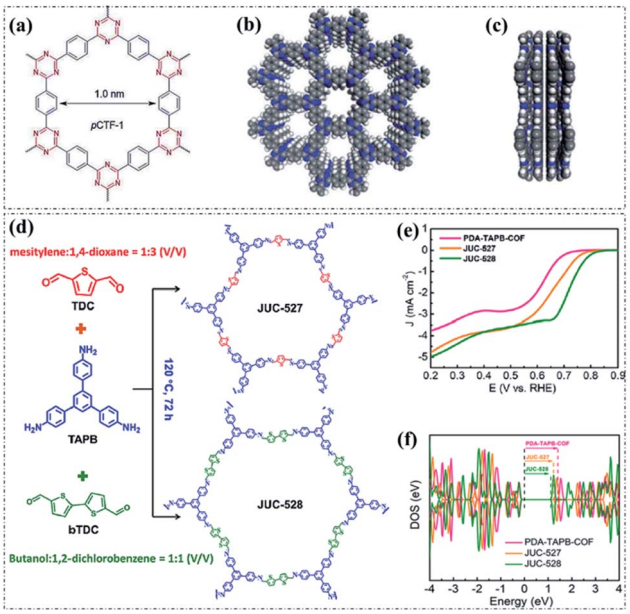


Fig. 2 The molecular structure (a) and space-filling diagrams (b and c) of pyrolysis-free CTFs: top view (b) and side view (c). C: gray, N: blue, H: white. Reproduced with permission from ref. 81, Copyright 2018 Wiley-VCH. (d) The synthesis and structures of JUC-527 and JUC-528. (e) LSV curves of PDA-TAPB-COF, JUC-527, and JUC-528 in 0.1 M KOH solution. (f) Calculated DOS diagram for PDA-TAPB-COF, JUC-527, and JUC-528. Reproduced with permission from ref. 77, Copyright 2020, American Chemical Society.

(both with the pentacyclic thiophene-S groups), showed obviously improved electrocatalytic ORR performance than the thiophene-free COFs (PDA-TAPB-COF; control sample).[77] Notably, the MFTS-COFs with higher proportions of thiophene-S (JUC-528) presented the best electrocatalytic ORR activity under alkaline conditions as revealed in Fig. 2e, indicating that the enhancement of the heteroatom concentration through rational selection and introduction of monomers have a positive effect on the electrocatalytic ORR activity. Density functional theory (DFT)-based simulations demonstrated that JUC-528 possesses the narrowest band gap (Fig. 2f), further supporting that the thiophene-S groups provided the positive ORR electrocatalytic capability. Besides, the as-prepared JUC-528 also showed an excellent long-term durability and outstanding structural stability with only a 7% loss after 25 h of continuous testing. It should be noted that conductive acetylene black was employed to increase the electrical conductivity of the system during the electrochemical measurements in this study. This work offers conducive information of the exact structure of active sites for pyrolysis-free COFs and provides a new route to design and develop high-performance oxygen electrocatalysts through precise and controllable incorporation of heteroatom active sites. The representative metal-free pyrolysis-free COF-based materials for oxygen electrocatalysis are summarized in Table 3.

Besides, the electrocatalytic selectivity can also be simply tuned by doping heteroatoms to alter the electronic structures through the whole backbones of pyrolysis-free COFs. A typical example recently reported by Li and co-authors proposed that the incorporation of electron-deficient thiazolo[5,4-*d*]thiazole into a viologen-based COF leads to partially positively charged carbon atoms that can serve as active sites and improve $O_2$ adsorption, resulting in a high $H_2O_2$ selectivity (92%) when used as an electrocatalyst for the ORR under alkaline conditions.[83] Furthermore, the $H_2O_2$ selectivity could be efficiently adjusted by the halide counteranion ($F^-$, $Cl^-$, $Br^-$, and $I^-$) exchange. As a consequence, the presence of F counteranion delivers a highest $H_2O_2$ selectivity (98.5%). DFT-based calculations demonstrated that the $H_2O_2$ selectivity of the obtained COFs is closely related to the electronegativity of the corresponding halide counteranion (F > Br > Cl > I). As can be seen in Fig. 3a and b, the binding energy of *OOH that dominates the $H_2O_2$ selectivity increases along with the electronegativity (F > Cl > Br > I), so that the $2e^-$ ORR activity of the obtained COFs follows the same order.

### 3.3 Metal-free pyrolysis-free COFs for the electrocatalytic OER

In addition to the electrocatalytic ORR, only a few reports are available for metal-free pyrolysis-free COF-based materials toward the electrocatalytic OER. This is mainly due to the generally inferior intrinsic activity of the incorporated heteroatoms. Interestingly, a recently reported study guided by theoretical calculation proposed a novel planar phenazine-linked COF (COF-$C_4N$) with appropriate CN stoichiometry, N position, and band structures for an efficient electrocatalytic OER (Fig. 3c and d).[84] The COF-$C_4N$ displayed both a low overpotential ($E_{j10}$) of 349 mV at 10 mA $cm^{-2}$ and a small Tafel slope of 64 mV $dec^{-1}$ under alkaline conditions (Fig. 3e and f). The combination of theoretical and experimental results demonstrated that the superior OER activity can be collectively ascribed to the high crystallinity, excellent stability, suitable band structure, and highly active C active sites. This work

Table 3 Summary of representative metal-free pyrolysis-free COF-based materials as catalysts for oxygen electrocatalysis

| Materials | Strategy | Active sites | Electrolyte | $E_{onset}$ (V *vs.* RHE) | $E_{1/2}$ (V *vs.* RHE) | *n* | $E_{j10}$ (mV *vs.* RHE) | Ref. |
|---|---|---|---|---|---|---|---|---|
| JUC-528 | Heteroatom introduction | Thiophene-S | 0.1 M KOH | 0.82 | 0.70 | 3.81 | — | 77 |
| JUC-527 | Heteroatom introduction | Thiophene-S | 0.1 M KOH | 0.77 | 0.63 | 3.46 | — | 77 |
| CTFs | Heteroatom introduction | Pyridinic-N | 0.1 M KOH | 0 (*vs.* SCE) | — | 3.6 | — | 80 |
| PTM-CORF | — | PTM radical | 0.1 M KOH | — | 0.671 | 3.89 | — | 82 |
| COF-$C_4N$ | Heteroatom introduction | C atoms | 1.0 M KOH | — | — | — | 349 | 84 |
| C4-SHz COF | Heteroatom introduction | N atoms | 1.0 M KOH | 1.50 | — | — | 320 | 85 |

 

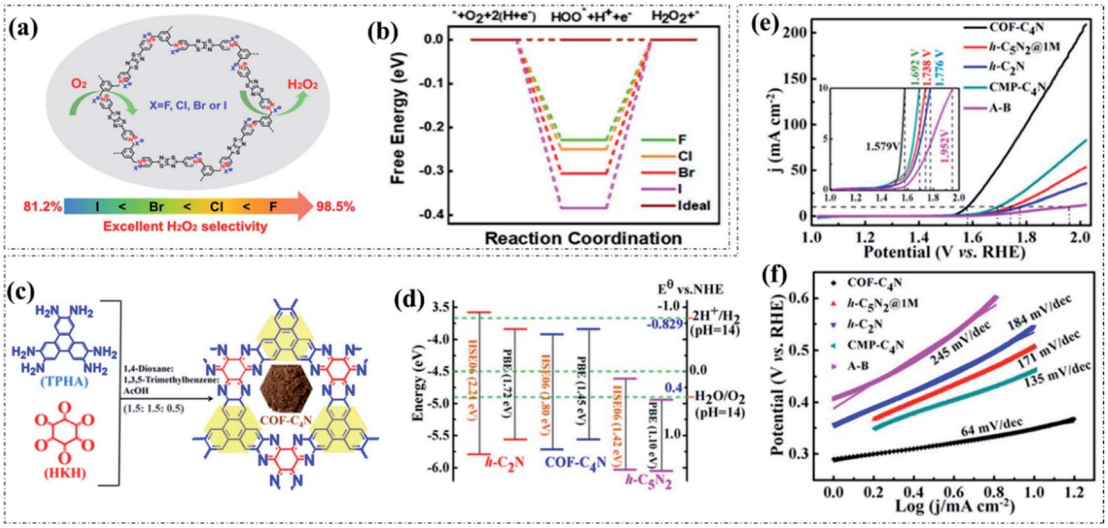


Fig. 3 (a) The molecular structure and excellent $H_2O_2$ selectivity of BPyTTz-COP:X (X = F, Cl, Br, and I). (b) Relative energy profiles for the ORR processes on BPyTTz-COP:X (X = F, Cl, Br, and I). Reproduced with permission from ref. 83, Copyright 2020, American Chemical Society. (c) The synthesis and molecular structure of COF-$C_4N$. (d) The calculated band structures of h-$C_2N$, COF-$C_4N$, and h-$C_5N_2$. (e) LSV curves and the corresponding (f) Tafel plots of various OER electrocatalysts in 1.0 M KOH solution. Reproduced with permission from ref. 84, Copyright 2019, American Chemical Society.

represents a significant progress in the construction of metal-free pyrolysis-free COF-based oxygen electrocatalysts.

Another study reported by Mondal and coworkers proposed and synthesized a new thiadiazole-based COF (C4-SHz COF) through a Schiff-base condensation polymerization between 1,3,5-tris(4-formylphenyl)benzene (C4–CHO) and 2,5-dihydrazinyl-1,3,4-thiadiazole (SHz), as can be seen in Fig. 4a and b.[85] In this work, a supercritical carbon dioxide treatment (Fig. 4c) was employed to activate the as-obtained C4-SHz COF, ensuring a well-defined molecular stacked framework structure and ultra-high specific surface area (1224 $m^2\ g^{-1}$). As a result, the C4-SHz COF as an electrocatalyst exhibited outstanding OER activity (onset overpotential of 270 mV, $E_{j10}$ of 320 mV, and Tafel slope of 39 mV $dec^{-1}$) under alkaline conditions (Fig. 4d and e), which is comparable to that of the recently developed transition metal-based materials. The excellent performance can be attributed to the superior structure (*e.g.*, high specific surface area, abundant porosity, and extended π-conjugation) enabled fast charge and mass transport. This work also corroborates the promising potential of metal-free pyrolysis-free COF-based materials for the electrocatalytic OER.

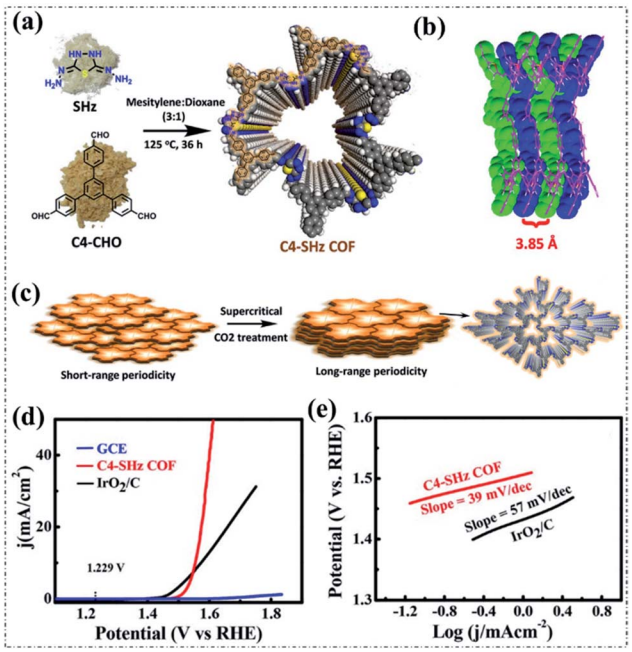


Fig. 4 (a and b) The synthesis and structure of C4-SHz COF. (c) The conversion from short- to long-range periodicity through supercritical carbon dioxide treatment. (d) LSV curves and the corresponding (e) Tafel plots of the OER electrocatalysts in 1.0 M KOH solution. Reproduced with permission from ref. 85, Copyright 2020, American Chemical Society.

## 4. Non-noble metal site-containing pyrolysis-free COFs for oxygen electrocatalysis

### 4.1 The vital role of non-noble metal sites in oxygen electrocatalysis

Although the reasonable incorporation of heteroatoms in pyrolysis-free COFs can effectively create high-efficiency active sites, the performance of metal-free pyrolysis-free COF-based materials in oxygen electrocatalysis still cannot meet the requirements of practical applications in the aforementioned sustainable electrochemical energy technologies. Therefore, it is urgent to further improve the electrocatalytic performance of pyrolysis-free COF-based materials. The incorporation of non-noble metals represents a promising strategy to engineer pyrolysis-free COF-based materials and significantly improve their performance for oxygen electrocatalysis.

As early as in 1964, researchers discovered that the non-noble metal phthalocyanine with an M–$N_4$ (M = Fe, Co, *etc.*) configuration showed obvious activity for oxygen electrocatalysis, indicating that non-noble transition metal-based atoms can be regarded as high-efficiency active sites toward oxygen electrocatalysis.[86] On the basis of this consensus, both the carbon-based M–N–C (M = Fe, Co, *etc.*) electrocatalysts prepared by high-temperature pyrolysis and the well-defined M–$N_4$ (M = Fe, Co, *etc.*) configuration-containing pyrolysis-free polymer-based materials have been proposed and widely studied in the field of oxygen electrocatalysis.[87–92] In fact, the reason for the significantly improved electrocatalytic activity can be fundamentally ascribed to the unique d orbital structure of these transition metal sites, which ensures appropriate adsorption of oxygenated intermediates and facilitates the further conversion of these intermediates. Besides, another possible mechanism accounting for activity improvement is closely related to neighbouring carbon atoms.[93] Generally, the incorporated transition metal sites deliver significantly improved electrocatalytic activity, and neighbouring carbon atoms play a role in synergistic enhancement. DFT-based simulation results theoretically support the above statement that neighbouring carbon atoms possess appropriate oxygen adsorption Gibbs free energy, signifying improved interactions between these carbon atoms and the oxygenated intermediates.[94] Compared with traditional carbon-based M–N–C materials, pyrolysis-free COF-based materials eliminate high-temperature pyrolysis and possess well-defined metal active sites and abundant natural pore structures with an equivalent chemical environment, favouring the study of electrocatalytic mechanisms.

### 4.2 Metallomacrocycle-containing pyrolysis-free COFs for oxygen electrocatalysis

There are generally two approaches to create non-noble transition metal active sites in pyrolysis-free COF-based materials. The first approach involves the reasonable selection of metal-chelating monomers (*e.g.*, porphyrin and phthalocyanine) and construction of metallomacrocycle-based pyrolysis-free COFs, such as metallophthalocyanine- and metalloporphyrin-based pyrolysis-free COFs. It is worth noting that the non-noble transition metal atoms can be tightly anchored into these judiciously selected metal-chelating monomers, forming a large number of well-defined M–$N_4$ active sites with an equal local coordination environment. It has already been well acknowledged that M–$N_4$ active sites deliver a more positive effect on the performance of oxygen electrocatalysis than the aforementioned heteroatom-incorporation strategy. This is mainly due to the highly active M–$N_4$ sites where hydroxyl intermediates could be effectively absorbed and electrons could be quickly transferred; however, specific analyses should be conducted to ascertain the effects of different types of metal sites. In the following, we will briefly present the recent advances of these common metallomacrocycle-based pyrolysis-free COFs as catalysts for oxygen electrocatalysis. The representative metal-containing pyrolysis-free COF-based materials for oxygen electrocatalysis are summarized in Table 4.

In principle, the highly conjugated structure of porphyrin provides a considerable electrocatalytic activity due to the relatively high electronic mobility and low work function.[95,96] More importantly, in terms of the structural composition, the macrocyclic porphyrin structure composed of four pyrrole groups bonded together by methine bridges could offer a suitable region for anchoring the transition metal sites to produce abundant well-defined M–$N_4$ active sites. As a consequence, the porphyrin structure possesses great potential for the design of highly effective oxygen electrocatalysts. Recently, Lin *et al.* theoretically simulated a series of metalloporphyrin-based pyrolysis-free COFs (Fig. 5a) using various 3d transition metal atoms and systematically investigated their ORR and OER activities.[97] Following the results of first-principles calculations, they proposed that both the configuration energy (CE) and crystal field stabilization energy (CFSE) can serve as intrinsic descriptors to represent the inherent 3d orbital energy of these selected 3d non-noble transition metals. On the basis of their proposed theory, only when the value of CFSE < −11, the corresponding metalloporphyrin-based pyrolysis-free COF follows the desired $4e^-$ pathway and

Table 4 Summary of representative metal-containing pyrolysis-free COF-based materials as catalysts for oxygen electrocatalysis

| Materials | Strategy | Active sites | Electrolyte | $E_{onset}$ (V *vs.* RHE) | $E_{1/2}$ (V *vs.* RHE) | $n$ | $E_{j10}$ (mV *vs.* RHE) | Ref. |
|---|---|---|---|---|---|---|---|---|
| FeSAs/PTF | Metal incorporation | Fe–$N_4$ | 0.1 M KOH | 1.01 | 0.87 | 3.88 | — | 98 |
| | | | 0.1 M $HClO_4$ | 0.89 | ≈0.75 | 3.99 | | |
| Co-PDY | Metal incorporation | Co–$N_4$ | 1.0 M KOH | — | — | — | 270 | 99 |
| Co-PyPc NSs | Metal incorporation | Co–$N_4$ | 0.1 M KOH | 0.974 | 0.815 | 3.47 | — | 101 |
| CoCMP | Metal incorporation | Co–$N_4$ | 0.1 M KOH | 1.57 | — | — | 610@13 mA $cm^{-2}$ | 102 |
| $COF_{BTC}$ | Metal incorporation | Fe–$N_4$ | 0.1 M KOH | 0.965 | ≈0.90 | — | — | 103 |
| Cu-CTF | Metal incorporation | Cu sites | Phosphate buffer (pH = 7) | 0.81 | ≈0.60 | 3.75–3.95 | — | 108 |
| | | | 0.1 M NaOH | 0.91 | ≈0.77 | — | | |
| Co-TpBpy | Metal incorporation | Co sites | Phosphate buffer (pH = 7) | — | — | — | 400@1 mA $cm^{-2}$ ≈520 | 109 |
| Macro-TpBpy-Co | Metal incorporation | Co sites | 0.1 M KOH | — | — | — | 380 | 110 |
| TpBpy-Co | Metal incorporation | Co sites | 0.1 M KOH | — | — | — | 430 | 110 |
| $Ni_{0.5}Fe_{0.5}$@COF-$SO_3$ | Metal incorporation | Ni and Fe sites | 1.0 M KOH | — | — | — | 308 | 111 |
| $Co_{0.5}V_{0.5}$@COF-$SO_3$ | Metal incorporation | Co and V sites | 1.0 M KOH | — | — | — | 318 | 112 |

 

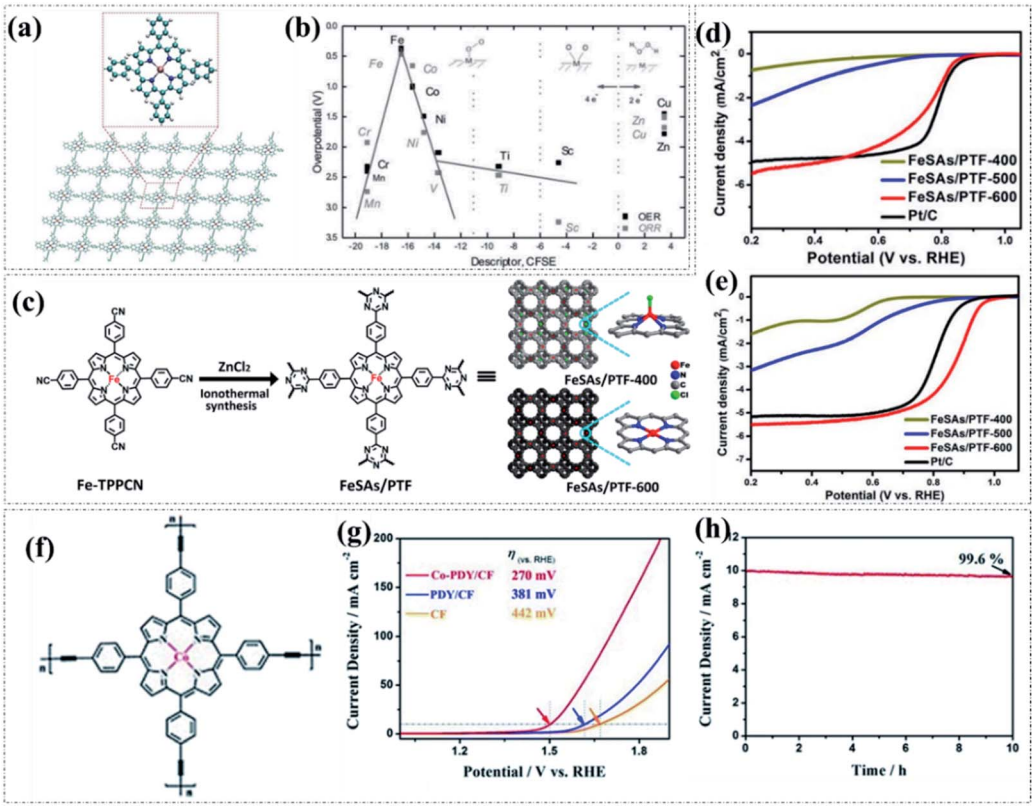


Fig. 5 (a) The molecular structure of transition metal-incorporated COFs. (b) The relationship between ORR/OER overpotentials and the proposed CFSE in $4e^-$ reactions. Reproduced with permission from ref. 97, Copyright 2017, Wiley-VCH. (c) The synthesis and molecular structure of FeSAs/PTF. LSV curves of the ORR electrocatalysts in (d) 0.1 M $HClO_4$ and (e) 0.1 M KOH solutions. Reproduced with permission from ref. 98, Copyright 2018, American Chemical Society. (f) The molecular structure of Co-PDY. (g) LSV curves of the OER electrocatalysts in 1.0 M KOH solution. (h) Chronopotentiometry curve of Co-PDY/CF for the OER at 1.50 V (*vs.* RHE). Reproduced with permission from ref. 99, Copyright 2019, Royal Society of Chemistry.

exhibits high electrocatalytic activity for the ORR and OER, as displayed in Fig. 5b. Accordingly, the electrocatalytic activity of the ORR and OER actually heavily depends on the type of 3d transition metal atom. Notably, Fe- and Co-containing metalloporphyrin-based pyrolysis-free COFs as electrocatalysts possess the best ORR and OER activity. This work provides researchers important theoretical basis for the estimation of the electrocatalytic activity of transition metal atom-incorporated pyrolysis-free COF-based materials. In terms of experimental research, most recently, Yi and coworkers employed a feasible ionothermal strategy (Fig. 5c) to prepare the atomically dispersed Fe–$N_4$ site-containing porphyrinic triazine-based COF (FeSAs/PTF) with a high Fe loading amount (up to 8.3 wt%).[98] The optimized FeSAs/PTF-600 displayed highly efficient activity and excellent durability for the electrocatalytic ORR in both acidic and alkaline environments (Fig. 5d and e) as a result of the high-density Fe–$N_4$ active sites, well-ordered frameworks, and high electrical conductivity. Specifically, the as-synthesized FeSAs/PTF-600 exhibited a high $E_{1/2}$ of 0.87 V in a 0.1 M KOH solution which is among the best reported values of carbon-based electrocatalysts. Furthermore, in a 0.1 M $HClO_4$ solution, the FeSAs/PTF-600 also displayed considerable performance with an $E_{1/2}$ of about 0.75 V. This work offers an effective approach to the design and preparation of metal-containing pyrolysis-free COFs for oxygen electrocatalysis. In another study, Huang *et al.* designed and prepared a Co–$N_4$ site-containing metalloporphyrin-based graphdiyne analogue (Co-PDY) through a Glaser–Hay coupling reaction on copper foam.[99] The obtained Co-PDY is composed of periodically repeating units of Co-coordinated phenyl-porphyrin connected with four butadiyne linkages, thus possessing a unique π-conjugated structure which could ensure fast electron transfer (Fig. 5f). Notably, the employed copper foam (CF) as a robust 3D conductive substrate in this work offers the obtained Co-PDY/CF significantly improved OER activity and excellent durability. As a result, the prepared Co-PDY/CF delivered an $E_{j10}$ of 270 mV under alkaline conditions, which is significantly lower than those of the bare CF (442 mV) and the control sample PDY/CF (381 mV) (Fig. 5g). After 10 h of continuous testing, only a 0.4% loss of OER current can be observed, indicating a superior long-term durability of Co-PDY/CF (Fig. 5h).

Similarly, the fully π-conjugated phthalocyanine enabled superior structural stability and electronic conductivity also make it stand out as a unique structural unit for building metallophthalocyanine-based COFs as pyrolysis-free electrocatalysts for oxygen electrocatalysis.[100] Recently, metallophthalocyanine-based pyrolysis-free COFs have emerged as a potential candidate to be used as oxygen electrocatalysts in practical application due to their superior electrocatalytic

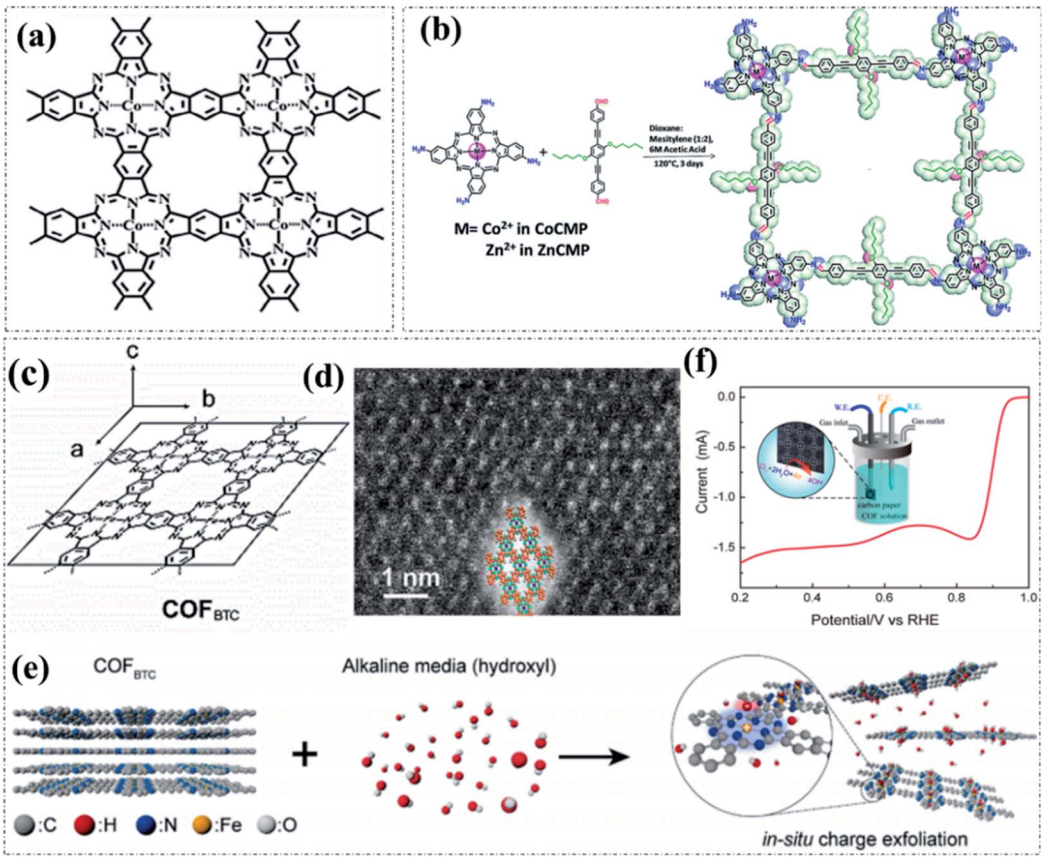


Fig. 6 (a) The molecular structure of Co-PyPc NSs. Reproduced with permission from ref. 101, Copyright 2019, Springer. (b) The synthesis and structure of CoCMP. Reproduced with permission from ref. 102, Copyright 2018, Royal Society of Chemistry. (c) The molecular structure and (d) STEM image of crystalline $COF_{BTC}$. (e) Exfoliation and dissolution route to $COF_{BTC}$ in alkaline media. (f) LSV curve of $COF_{BTC}$ solution with carbon paper as the electrodes. Inset: scheme for the detailed operation for the measurements. Reproduced with permission from ref. 103, Copyright 2019, American Chemical Society.

performance. The high-efficiency activity of metallophthalocyanine-based pyrolysis-free COFs towards the ORR has been experimentally validated. As reported, the cobalt-phthalocyanine nanosheets (Co-PyPc NSs) (Fig. 6a) exhibited an excellent ORR electrocatalytic activity with the desired $4e^-$ pathway, delivering both a high onset potential ($E_{onset}$) of 0.974 V and a half-wave potential ($E_{1/2}$) of 0.815 V under alkaline conditions, comparable to those of the commercially available Pt/C electrocatalyst.[101] A similar study by Singh *et al.* reported a Co–$N_4$ site-containing phthalocyanine-based COF (CoCMP) through a Schiff-base condensation reaction (Fig. 6b).[102] The obtained CoCMP showed an efficient OER activity with an $E_{onset}$ of 1.57 V, overpotential of 610 mV (at 13 mA $cm^{-2}$), and Tafel slope of 87 mV $dec^{-1}$ in alkaline media. Notably, the CoCMP maintained a consistent electrocatalytic activity even after 1000 cycles, indicating a superior durability. In addition, the construction of a-few-layer-thick pyrolysis-free COFs is of particular interest to reduce the π–π stacking of pyrolysis-free COFs, thus improving the utilization of active sites and boosting the mass transport. Recently, Xiang *et al.* reported the exfoliation of a metallophthalocyanine-based pyrolysis-free COF ($COF_{BTC}$; Fig. 6c and d) into monolayers to further improve the electrocatalytic ORR activity.[103] As displayed in Fig. 6e, the *in situ* exfoliation of the iron phthalocyanine COF in an alkaline solution *via* the insertion of hydroxide groups into the stacking layers can obviously increase the number of exposed active sites. In addition, the hydroxide groups can also absorb onto the positively charged Fe sites, leading to the formation of a stable solution. The as-prepared soluble COF contains well-defined Fe–$N_4$ active sites and highly conjugated structures, showing a small work function of 4.84 eV and superior electrocatalytic performance for the ORR with an $E_{1/2}$ of ~900 mV (Fig. 6f). This work represents an important future research direction to reduce the π–π stacking of pyrolysis-free COFs, boost the mass transport and increase the active site utilization.

### 4.3 Incorporating non-noble metal sites by post-modification

The second approach to incorporate non-noble transition metal active sites in pyrolysis-free COF-based materials mainly involves post-treatment processes. In most cases, the pyrolysis-free COFs created using metal-free structural units actually do not contain high-efficiency metal active sites. Therefore, these metal-free pyrolysis-free COF-based materials usually only showed inferior electrocatalytic activities. Accordingly, metal

 

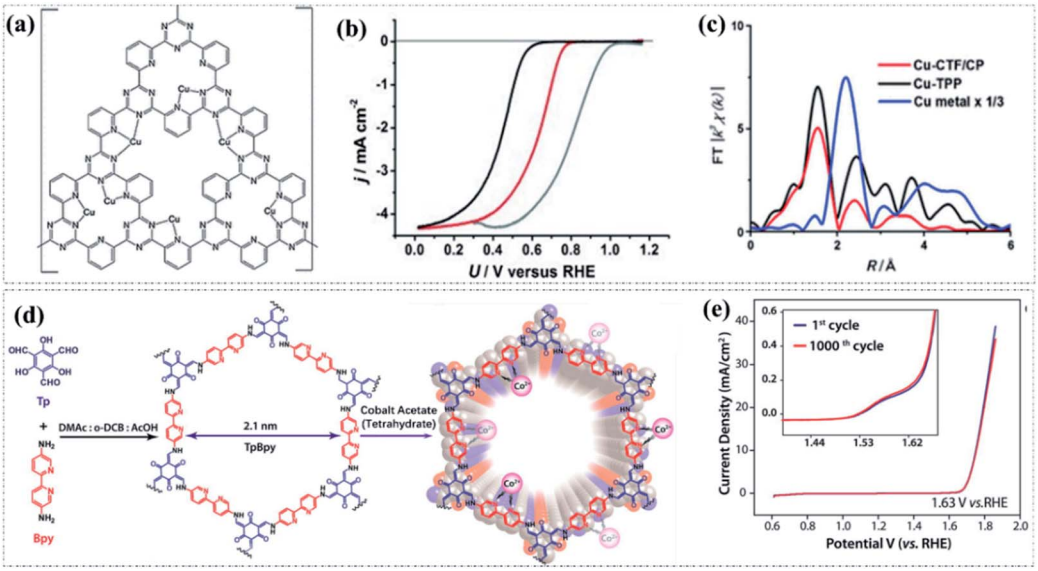


Fig. 7 (a) Schematic representation of Cu-CTF. (b) $k^3$-weighted Fourier transform of EXAFS spectra of the Cu K edge for Cu-CTF/CP (red), Cu-TPP (black), and Cu metal (blue). (c) LSV curves of Cu-CTF/CP (red), CTF/CP (black), and Pt/C (gray) in a phosphate buffered solution (pH 7). Reproduced with permission from ref. 108, Copyright 2015, Wiley-VCH. (d) The synthesis and molecular structure of Co-TpBpy. (e) LSV curves of Co-TpBpy before and after 1000 cycles (inset shows the enlarged view) in a phosphate buffered solution (pH 7). Reproduced with permission from ref. 109, Copyright 2016, American Chemical Society.

active sites can be incorporated into the predesigned metal-free pyrolysis-free COFs *via* some post-treatment processes, such as absorption and cation exchange.[104–107] For instance, Iwase *et al.* recently reported a Cu-modified CTF material (Fig. 7a) as a catalyst for the ORR by taking advantage of the strong interaction between Cu ions and pyridinic-N sites.[108] The incorporation of Cu atoms causes a significant decline in the overpotential of around 0.2 V and delivers an $E_{onset}$ of 0.81 V in a neutral solution, signifying a positive role of the incorporated Cu atom sites (Fig. 7b). The improved ORR performance is attributed to the produced coordination unsaturated Cu atoms (Fig. 7c), which can provide a more accessible d orbital, resulting in stronger interaction with $O_2$ and promoting the O–O bond breaking. In another study, a Co-modified bipyridine-containing COF (Co-TpBpy) was prepared through a Schiff-base condensation reaction between 1,3,5-trifomylphloroglucinol (Tp) and 2,20-bipyridine-5,50-diamine (Bpy) followed by a post-treatment process to incorporate Co metal sites (Fig. 7d).[109] The bipyridine moieties that are periodically present in the skeleton of the TpBpy COF are capable of strong coordination with cobalt ions due to the bidentate chelation, therefore producing abundant well-defined Co–N active sites. Benefiting from the highly accessible surface area (450 $m^2\ g^{-1}$) and the incorporation of abundant Co–N active sites, the obtained Co-TpBpy displayed a reasonable electrocatalytic OER activity with an overpotential of 400 mV at 1 mA $cm^{-2}$ and a calculated $E_{j10}$ of about 520 mV in neutral pH media (Fig. 7e). Besides, the obtained Co-TpBpy also exhibited a good durability with nearly 94% retention of the OER current after 1000 cycles of potential scanning mainly attributed to the synergetic effect of the rich porosity and presence of abundant Co–N sites in the skeleton of COFs. It is worth noting that conductive acetylene black was employed to improve the electrical conductivity of Co-TpBpy during the electrochemical measurements in this work.

In addition to the incorporation of highly active metal sites, the mass transport of gas (oxygen)/liquid (electrolyte) also plays a crucial role in the process of oxygen electrocatalysis. Even though the rich micropores and/or small mesopores of pyrolysis-free COFs could offer high specific surface area and therefore high density of well-defined active sites, they are too small to ensure fast mass transport throughout the skeleton. In this regard, the design of hierarchically porous structured pyrolysis-free COFs by introducing additional large mesopores and/or macropores into pyrolysis-free COFs is considered to be a highly feasible approach to improve mass transport. As recently reported by Zhao and coworkers, polystyrene spheres (PSs) can be used as a facile hard template to introduce hierarchically porous structures in pyrolysis-free COFs (Fig. 8a).[110] The obtained macroporous COFs possess high crystallinity and high specific surface area. The enhanced mass transport and therefore the activity were verified by evaluating the performance of a Co-coordinated bipyridine-based COF (macro-TpBpy-Co) as an electrocatalyst for the OER (Fig. 8b and c). The macro-TpBpy-Co exhibited significantly improved OER performance under alkaline conditions with both a lower $E_{j10}$ of 380 mV and a smaller Tafel slope of 54 mV $dec^{-1}$ compared with those of the purely microporous COF (TpBpy-Co) (Fig. 8d and e), which can be undoubtedly ascribed to the enhanced mass transport and the exposure of more accessible active sites.

In addition, to further improve the utilization of the metal sites and stability, bimetallic site-incorporated pyrolysis-free COFs have been proposed and validated to be feasible for the electrocatalytic OER. Gao and coworkers recently reported a novel post-treatment approach by cation exchange to prepare

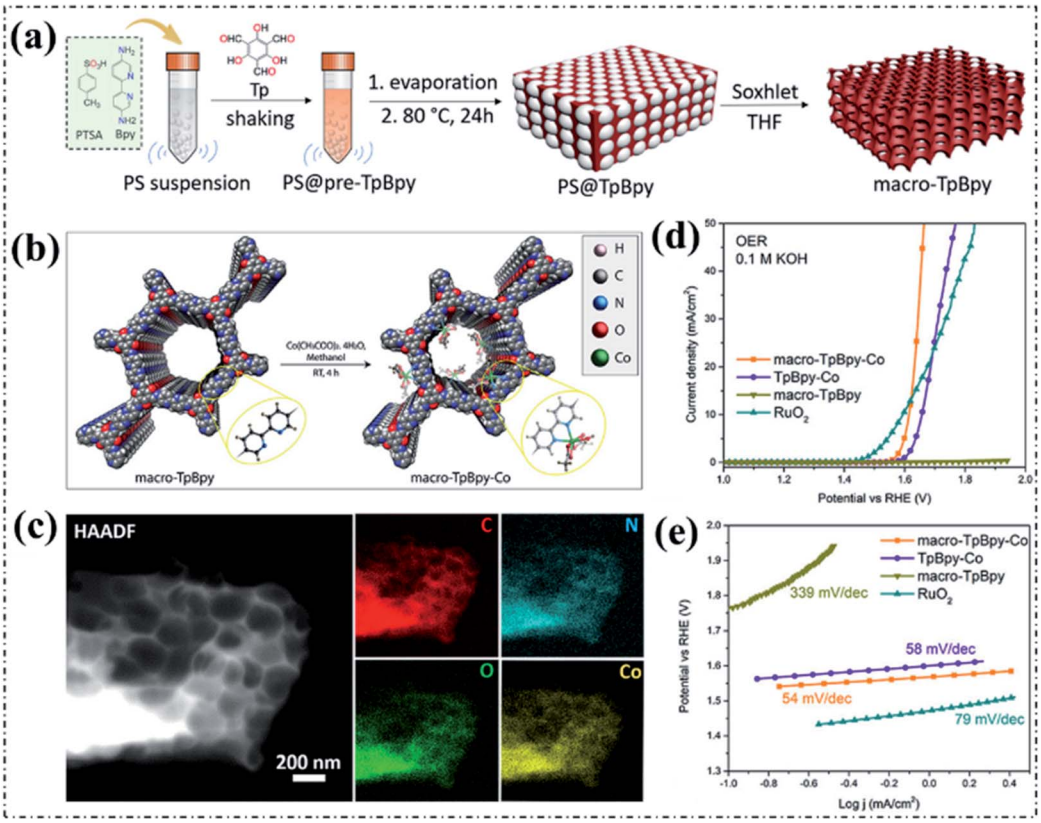


Fig. 8 (a) The synthesis of macro-TpBpy in the presence of PSs. (b) The post-treatment synthesis and structure of macro-TpBpy-Co. (c) HAADF-STEM images of macro-TpBpy-Co and the corresponding element mapping images. (d) LSV curves and the corresponding (e) Tafel plots of the OER electrocatalysts in 0.1 M KOH solution. Reproduced with permission from ref. 110, Copyright 2019, American Chemical Society.

bimetallic Ni/Fe site-incorporated pyrolysis-free COFs ($Ni_x$-$Fe_{1-x}$@COF-$SO_3$) as electrocatalysts for the OER (Fig. 9a).[111] The optimized bimetallic $Ni_{0.5}Fe_{0.5}$@COF-$SO_3$ obtained by adjusting the ratio of Ni/Fe displayed an $E_{j10}$ of 308 mV under alkaline conditions, which is significantly lower than those of monometallic site-incorporated pyrolysis-free COFs (*i.e.*, Ni@COF-$SO_3$ and Fe@COF-$SO_3$) and even better than that of the commercial $IrO_2$ electrocatalyst (327 mV) (Fig. 9b and c). The excellent OER performance can be attributed to the further improved intrinsic activity of the incorporated bimetallic Ni/Fe sites due to the electronic synergistic effects and the unique structure of the pyrolysis-free COFs. Similarly, $Co_xV_{1-x}$@COF-$SO_3$ electrocatalysts also have been prepared through the same approach and the optimized $Co_{0.5}V_{0.5}$@COF-$SO_3$ delivered an outstanding OER performance with an $E_{j10}$ of only 300 mV under alkaline conditions.[112] The above studies pave a new avenue to design and construct high-performance metal-incorporated pyrolysis-free COF-based electrocatalysts.

## 5. The combination of pyrolysis-free COFs with conductive supports for oxygen electrocatalysis

In addition to the construction of well-designed high-efficiency active sites and improvement of the exposure of these active sites, the electronic conductivity of pyrolysis-free COF-based materials is also highly pivotal in oxygen electrocatalysis. Due to the relatively poor electrical conductivity, pyrolysis-free COFs can be hybridized with some high-surface-area conductive supporting materials (*e.g.*, graphene, CNTs and carbon nanoparticles) that provide abundant conducting channels and more effective surface area for forming pyrolysis-free COF-based hybrid systems.[24,25,42–44] To ensure close contact between the pyrolysis-free COFs and these conductive materials, the direct growth of crystalline COFs on the surface of a substrate as thin films seems to be the best way for building heterostructures and achieving improved electrical conductivity and mechanical stability. Table 5 summarizes the representative pyrolysis-free COF/conductive support hybrids recently reported for oxygen electrocatalysis.

### 5.1 Pyrolysis-free COFs/CNTs for oxygen electrocatalysts

Due to the high electronic conductivity, large specific surface area and strong stability, CNTs have been recently used as both a template and current collector to guide pyrolysis-free COF growth, prevent the excessive stacking of pyrolysis-free COF layers, increase the exposed active sites, and improve the electronic conductivity of the whole pyrolysis-free COF-based hybrid systems. Notably, the synergistic effect of π-stacking interactions between the CNTs and the thin films of pyrolysis-free COFs has also been proposed to account for the partial

 

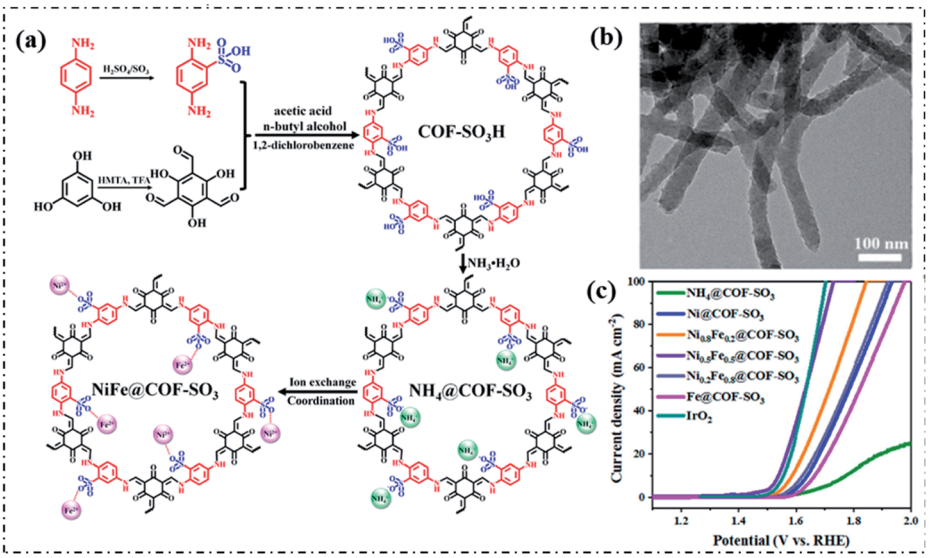


Fig. 9 (a) Schematic illustration of the synthesis of $Ni_{0.5}Fe_{0.5}$@COF-$SO_3$. (b) TEM image of $Ni_{0.5}Fe_{0.5}$@COF-$SO_3$. (c) LSV curves of the OER electrocatalysts in 1.0 M KOH solution. Reproduced with permission from ref. 111, Copyright 2020, American Chemical Society.

Table 5 Summary of representative pyrolysis-free COF/conductive support hybrids as catalysts for oxygen electrocatalysis

| Materials | Strategy | Active sites | Electrolyte | $E_{onset}$ (V *vs.* RHE) | $E_{1/2}$ (V *vs.* RHE) | *n* | $E_{j10}$ (mV *vs.* RHE) | Ref. |
|---|---|---|---|---|---|---|---|---|
| CC-3 vdWHs | Conductive support hybridization | Thiophene-S | 0.1 M KOH | — | 0.828 | 3.86 | 389 | 113 |
| COP-$PSO_3$-Co-rGO | Conductive support hybridization | C atoms | 1.0 M KOH | 0.88 | ≈0.72 | 3.70 | — | 24 |
| pfSAC-Fe-0.2 | Conductive support hybridization | Fe–$N_4$ | 0.1 M KOH | — | 0.91 | 3.85–4.00 | — | 25 |
| MWNT-CoP | Conductive support hybridization | Co–$N_4$ | 0.5 M $H_2SO_4$ | — | — | Up to 3.93 | — | 43 |
| $(CoP)_n$-MWCNTs | Conductive supports hybridizing | Co–$N_4$ | 1.0 M KOH | — | — | — | 290@1 mA $cm^{-2}$ | 44 |
| CoCOF-Py-0.05rGO | Conductive support hybridization | Co–$N_4$ | 0.1 M KOH | 0.84 | 0.765 | 3.7–3.9 | — | 115 |

enhancement of electrocatalytic activity. Very recently, Liu *et al.* adopted an *in situ* wrapping strategy to form van der Waals heterostructures (vdWHs) by growing electrocatalytically active metal-free thienothiophene-containing COF shells with tuneable thickness around a highly conductive multiwalled CNT (MWCNT) core (CC-*X* vdWHs), as can be seen in Fig. 10a.[113] The optimized hybrid CC-3 vdWH with a COF shell thickness of 3 nm displayed an excellent ORR activity in an alkaline electrolyte with a high $E_{1/2}$ of 0.828 V and an electron transfer number of 3.86 (obtained from RRDE tests) (Fig. 10b and c). Besides, the CC-3 vdWH also exhibited a reasonable OER performance with an $E_{j10}$ of 389 mV under alkaline conditions. The strong n-type electronic interaction between the CNT cores and COF shells is assigned as the origin of the dramatically enhanced electrocatalytic performance, as revealed by the DFT calculations (Fig. 10d). In addition, Li and co-workers reported the construction of pyrolysis-free COF/CNT hybrids (CNT@POF (porphyrin covalent organic framework)) and studied their electrocatalytic activities in a Zn–air battery (Fig. 10e).[114] Compared with the pristine POF (with a dense spherical morphology), the POF coated on the surface of the CNTs displayed an ultra-thin thickness (Fig. 10f and g). The obtained Zn–air battery assembled with CNT@POF (Fig. 10h) delivered better performance than the commercial Pt/C electrocatalyst assembled device, revealing a considerable practical value. Apart from the alkaline electrolyte, pyrolysis-free COF/conductive support hybrids have also been applied under acid conditions. Recently, Hijazi *et al.* prepared a Co–$N_4$ site-containing porphyrin-based COF/MWCNT hybrid (MWNT-CoP) using MWCNTs as the template.[43] As a result of the cooperative effect of the π–π stacking interactions between the porphyrin-based pyrolysis-free COF and the MWNTs and the covalent links between the porphyrins, the obtained MWNT-CoP displayed superior ORR performance under acidic conditions with electron transfer numbers close to 4 (up to 3.93).

### 5.2 Pyrolysis-free COF/graphene for oxygen electrocatalysts

Reduced graphene oxide (rGO) has also been reported as a support to combine with pyrolysis-free COF-based materials. Xiang and co-workers reported the self-assembly of a porphyrin-based pyrolysis-free COF with rGO (COP-$PSO_3$-Co-rGO) (Fig. 11a) and studied the electrocatalytic ORR performance of the obtained hybrid system under alkaline conditions.[24] The electrical conductivity of the hybridized COP-$PSO_3$-Co-rGO is significantly increased by more than seven orders of magnitude compared with that of pure COPs. Accordingly, the

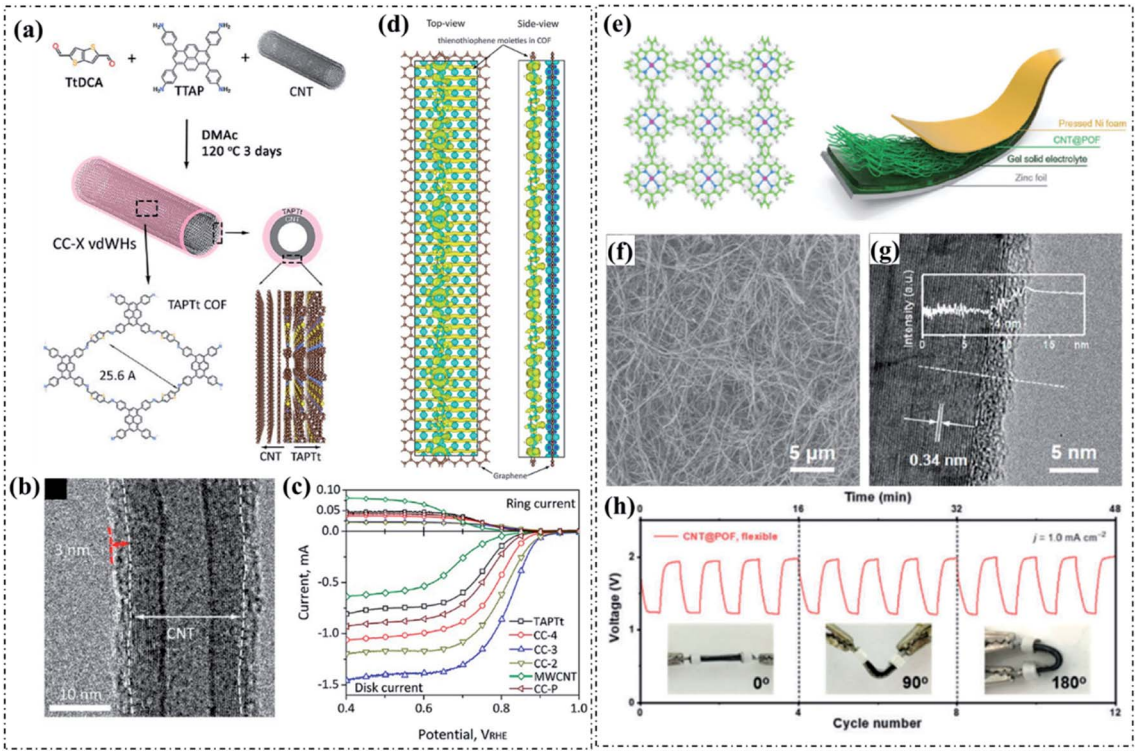


Fig. 10 (a) Schematic illustration of the synthesis of CC-*X* vdWHs. (b) TEM image of CC-3 vdWH. (c) LSV curves of the ORR electrocatalysts in 0.1 M KOH solution. (d) Calculated charge density difference profiles of CC-*X* vdWHs. Reproduced with permission from ref. 113, Copyright 2021, American Chemical Society. (e) The molecular structure of the POF and the illustration of the Zn–air battery (CNT@POF serves as the cathode). (f) SEM and (g) HRTEM images of CNT@POF, and the inset shows the contrast profile along the white dashed line. (h) Galvanostatic discharge–charge cycling curves at 1.0 mA $cm^{-2}$ under bending at 0°, 90°, and 180°, respectively. Reproduced with permission from ref. 114, Copyright 2018, Royal Society of Chemistry.

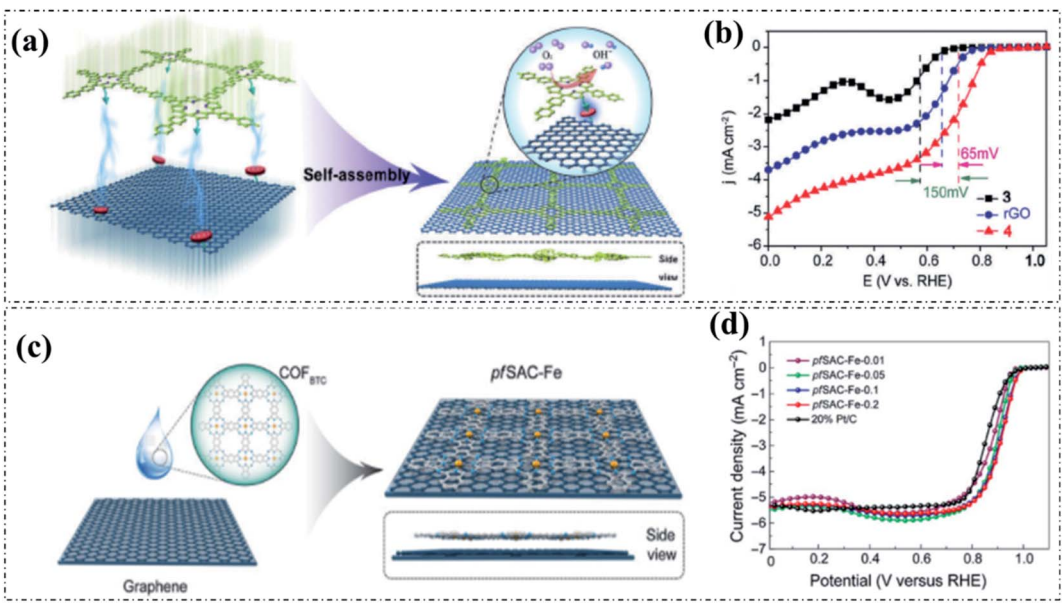


Fig. 11 (a) The synthesis of COP-$PSO_3$-Co-rGO. (b) The LSV curves of COP-$PSO_3$-Co-rGO and control samples (3 and 4 are COP-$PSO_3$-Co and COP-$PSO_3$-Co-rGO, respectively) in 1.0 M KOH solution. Reproduced with permission from ref. 24, Copyright 2018, Wiley-VCH. (c) The synthesis of pfSAC-Fe. (d) The LSV curves of pfSAC-Fe-X and Pt/C in 0.1 M KOH solution. Reproduced with permission from ref. 25, Copyright 2019, American Association for the Advancement of Science.

 

electrocatalytic ORR activity of COP-$PSO_3$-Co-rGO is markedly improved as a result of the synergistic effect between highly active COPs and highly conductive rGO (Fig. 11b). Moreover, an atomic-scale Fe-containing pyrolysis-free COF was also reported to hybridize with graphene *via* van der Waals interaction, as shown in Fig. 11c.[25] All of the as-prepared pfSAC-Fe hybrids showed excellent electrocatalytic activity for the ORR under alkaline conditions compared to the benchmark Pt/C (Fig. 11d). Meanwhile, the optimized sample pfSAC-Fe-0.2 delivered the best ORR activity with a high $E_{1/2}$ of 0.91 V and a kinetic current density 4 times higher than that of the commercial Pt/C electrocatalyst in 0.1 M KOH solution.

## 6. Conclusions and perspectives

As a unique type of crystalline porous polymer, pyrolysis-free COFs have emerged as both promising catalytic materials for electrochemical energy conversion applications and ideal platforms for electrocatalysis research due to their tunable porosity, predesigned building units, atomically precise structures, and programmable topological architectures. Clearly distinct from traditional carbon-based electrocatalysts prepared generally *via* a high-temperature pyrolysis process, the pyrolysis-free COF-based electrocatalysts simultaneously ensure the precise controllability of the material structure and active site configuration and retain the excellent electrocatalytic performance. A model electrocatalyst can be therefore reasonably proposed based on the clear structure–activity relationships of pyrolysis-free COF-based electrocatalysts, which makes the in-depth investigation of the active sites and reaction mechanisms easier. The engineering strategies including heteroatom introduction, non-noble metal site incorporation, and combination with high-surface-area conductive supports have been clearly verified to be effective for the improvement of the electrocatalytic performance. This review systematically summarizes the recent advances of pyrolysis-free COF-based materials as electrocatalysts for oxygen electrocatalysis. The pivotal roles of heteroatoms, non-noble metal sites and high-surface-area conductive supports in the electronic structure modulation and synergistic enhancement effect are carefully detailed.

Even though considerable progress has been obtained in creating pyrolysis-free COF-based materials for oxygen electrocatalysis, there are some urgent challenges that have not yet been solved. Therefore, future research needs to focus on the following several directions to further enhance the electrocatalytic performance of pyrolysis-free COF-based electrocatalysts to achieve large-scale practical applications:

1. More attention is required to be paid on the electrocatalytic mechanisms. Currently, the electrocatalytic mechanisms of carbon-based materials are still controversial mainly due to the unpredictable and poorly defined electrocatalytically active sites. With the rapid development of *in situ* characterization technologies, pyrolysis-free COF-based materials serving as model electrocatalysts could provide more insightful information on the structure–activity relationships. Therefore, continuous efforts are suggested to focus on the *in situ* characterization of pyrolysis-free COF-based materials during the electrocatalytic process. Based on this acquired new knowledge, more efficient electrocatalysts can be readily designed and constructed.

2. The intrinsic activity of active sites needs to be further improved, particularly in the case of acidic conditions. At present, the common pyrolysis-free COF-based electrocatalysts show considerable electrocatalytic performance only in alkaline electrolytes, while under acidic conditions, the pyrolysis-free COF-based electrocatalysts still cannot compete with the noble-metal-based benchmarks. Therefore, the development of high-efficiency active sites under acidic conditions plays an important role in the research of oxygen electrocatalysis and the reaction mechanisms in acidic electrolytes.

3. Great efforts are urgently needed towards the exploitation of 3D pyrolysis-free COF-based electrocatalysts. Until now, almost all of the reported pyrolysis-free COF-based electrocatalysts are 2D stacking structures. To further improve the exposure of the active sites and build more reasonable channels and pore microstructures, the synthesis of 3D pyrolysis-free COFs is highly recommended.

4. New and more convenient synthesis methods should be widely explored and developed. Even though various approaches have been proposed for the synthesis of pyrolysis-free COF-based electrocatalysts, most of these strategies are complicated and time-consuming. Besides, the large-scale production is still a very challenging task. Therefore, there is an urgent need to develop new and convenient synthesis methods.

5. The simultaneous incorporation of multiple electrocatalytically active sites into pyrolysis-free COF-based materials is highly desired to further improve the electrocatalytic activity and expand the functionality and application fields. The synergistic enhancement effect may play a vital role in further improving the electrocatalytic activity of pyrolysis-free COF-based materials incorporated with multiple active sites.

6. Ultra-thin lamellar pyrolysis-free COFs are highly desired and urgently needed towards application in oxygen electrocatalysis. More attention should be paid to the development of convenient exfoliation methods or preparation methods of ultra-thin pyrolysis-free COF films.

Overall, we would like to highlight that although these fascinating electrocatalysts are still in their infancy, their impressive electrocatalytic performance has revealed promising potential for large-scale use in the electrochemical energy conversion technologies. With the rapid development of this field, we believe that pyrolysis-free COF-based electrocatalysts are highly possible to become a research hotspot.

## Conflicts of interest

There are no conflicts to declare.

## Acknowledgements

This work was financially supported by the National Natural Science Foundation of China (52003300, 51973235, 51673061,

and 52173091) and the Fundamental Research Funds for the Central Universities (CZP19001).

## Notes and references

1 X. Cui, P. Xiao, J. Wang, M. Zhou, W. Guo, Y. Yang, Y. He, Z. Wang, Y. Yang, Y. Zhang and Z. Lin, *Angew. Chem., Int. Ed.*, 2017, **56**, 4488–4493.
2 L. Gao, X. Cui, Z. Wang, C. D. Sewell, Z. Li, S. Liang, M. Zhang, J. Li, Y. Hu and Z. Lin, *Proc. Natl. Acad. Sci. U. S. A.*, 2021, **118**, e2023421118.
3 X. Cui, W. Guo, M. Zhou, Y. Yang, Y. Li, P. Xiao, Y. Zhang and X. Zhang, *ACS Appl. Mater. Interfaces*, 2015, **7**, 493–503.
4 Q. Hu, X. Liu, B. Zhu, L. Fan, X. Chai, Q. Zhang, J. Liu, C. He and Z. Lin, *Nano Energy*, 2018, **50**, 212–219.
5 X. Cui, Y. Yang, Y. Li, F. Liu, H. Peng, Y. Zhang and P. Xiao, *J. Electrochem. Soc.*, 2015, **162**, F1415–F1424.
6 S. Chandrasekarana, D. Ma, Y. Ge, L. Deng, C. Bowen, J. Roscow, Y. Zhang, Z. Lin, R. Misra, J. Li, P. Zhang and H. Zhang, *Nano Energy*, 2020, **77**, 105080.
7 T. Wang, C. Yang, Y. Liu, S. M. Yang, X. Li, M. Yang, Y. He, H. Li, H. Chen and Z. Lin, *Nano Lett.*, 2020, **20**, 5639–5645.
8 T. Wang, Y. He, Y. Liu, F. Guo, X. Li, H. Chen, H. Li and Z. Lin, *Nano Energy*, 2020, **79**, 105487.
9 J. Zhang and L. Dai, *ACS Catal.*, 2015, **5**, 7244–7253.
10 W. T. Hong, M. Risch, K. A. Stoerzinger, A. Grimaud, J. Suntivich and Y. Shao-Horn, *Energy Environ. Sci.*, 2015, **8**, 1404–1427.
11 L. Gao, X. Cui, C. D. Sewell, J. Li and Z. Lin, *Chem. Soc. Rev.*, 2021, **50**, 8428–8469.
12 H. Wang, R. Liu, Y. Li, X. Lü, Q. Wang, S. Zhao, K. Yuan, Z. Cui, X. Li, S. Xin, R. Zhang, M. Lei and Z. Lin, *Joule*, 2018, **2**, 337–348.
13 X. Cui, L. Gao, S. Lei, S. Liang, J. Zhang, C. D. Sewell, W. Xue, Q. Liu, Z. Lin and Y. Yang, *Adv. Funct. Mater.*, 2021, **31**, 2009197.
14 W. Xue, Q. Zhou, X. Cui, S. Jia, J. Zhang and Z. Lin, *Nano Energy*, 2021, **86**, 106073.
15 H.-F. Wang, L. Chen, H. Pang, S. Kaskel and Q. Xu, *Chem. Soc. Rev.*, 2020, **49**, 1414–1448.
16 H. Cui, Z. Zhou and D. Jia, *Mater. Horiz.*, 2017, **4**, 7–19.
17 R. Kumar, S. Sahoo, E. Joanni, R. K. Singh, K. Maegawa, W. K. Tan, G. Kawamura, K. K. Kar and A. Matsuda, *Mater. Today*, 2020, **39**, 47–65.
18 C. D. Sewell, Z. Wang, Y.-W. Harn, S. Liang, L. Gao, X. Cui and Z. Lin, *J. Mater. Chem. A*, 2021, DOI: 10.1039/D1TA04511C.
19 Y.-W. Harn, S. Liang, S. Liu, Y. Yan, Z. Wang, J. Jiang, J. Zhang, Q. Li, Y. He, Z. Li, L. Zhu, H.-P. Cheng and Z. Lin, *Proc. Natl. Acad. Sci. U. S. A.*, 2021, **118**, e2014086118.
20 J. Duan, S. Chen, M. Jaroniec and S. Z. Qiao, *ACS Catal.*, 2015, **5**, 5207–5234.
21 X. Wang, G. Sun, P. Routh, D.-H. Kim, W. Huang and P. Chen, *Chem. Soc. Rev.*, 2014, **43**, 7067–7098.
22 X. Wang, Z. Li, Y. Qu, T. Yuan, W. Wang, Y. Wu and Y. Li, *Chem*, 2019, **5**, 1486–1511.
23 C.-X. Zhao, B.-Q. Li, J.-N. Liu and Q. Zhang, *Angew. Chem., Int. Ed.*, 2021, **60**, 4448–4463.
24 J. Guo, C.-Y. Lin, Z. Xia and Z. Xiang, *Angew. Chem., Int. Ed.*, 2018, **57**, 12567–12572.
25 P. Peng, L. Shi, F. Huo, C. Mi, X. Wu, S. Zhang and Z. Xiang, *Sci. Adv.*, 2019, **5**, eaaw2322.
26 S. Tao and D. Jiang, *CCS Chem.*, 2020, **2**, 2003–2024.
27 C. Mi, P. Peng and Z. Xiang, *Chin. Sci. Bull.*, 2020, **65**, 1348–1357.
28 P. Peng, Z. Zhou, J. Guo and Z. Xiang, *ACS Energy Lett.*, 2017, **2**, 1308–1314.
29 A. P. Cote, A. I. Benin, N. W. Ockwig, M. O'Keeffe, A. J. Matzger and O. M. Yaghi, *Science*, 2005, **310**, 1166–1170.
30 Z. H. Xiang and D. P. Cao, *J. Mater. Chem. A*, 2013, **1**, 2691–2718.
31 J. Li, X. Jing, Q. Li, S. Li, X. Gao, X. Feng and B. Wang, *Chem. Soc. Rev.*, 2020, **49**, 3565–3604.
32 Z. Xiang, D. Cao and L. Dai, *Polym. Chem.*, 2015, **6**, 1896–1911.
33 M. S. Lohse and T. Bein, *Adv. Funct. Mater.*, 2018, **28**, 1705553.
34 C. Y. Lin, D. Zhang, Z. Zhao and Z. Xia, *Adv. Mater.*, 2018, **30**, 1703646.
35 X. Cui, S. Lei, A. C. Wang, L. Gao, Q. Zhang, Yi. Yang and Z. Lin, *Nano Energy*, 2020, **70**, 104525.
36 M. Xiao, Y. Chen, J. Zhu, H. Zhang, X. Zhao, L. Gao, X. Wang, J. Zhao, J. Ge, Z. Jiang, S. Chen, C. Liu and W. Xing, *J. Am. Chem. Soc.*, 2019, **141**, 17763–17770.
37 Y. Han, Y. Wang, R. Xu, W. Chen, L. Zheng, A. Han, Y. Zhu, J. Zhang, H. Zhang, J. Luo, C. Chen, Q. Peng, D. Wang and Y. Li, *Energy Environ. Sci.*, 2018, **11**, 2348–2352.
38 X. Wang, A. Vasileff, Y. Jiao, Y. Zheng and S. Z. Qiao, *Adv. Mater.*, 2019, **31**, 1803625.
39 H. Ma, B. Liu, B. Li, L. Zhang, Y. G. Li, H. Q. Tan, H. Y. Zang and G. Zhu, *J. Am. Chem. Soc.*, 2016, **138**, 5897–5903.
40 Q. Xu, Y. Tang, X. Zhang, Y. Oshima, Q. Chen and D. Jiang, *Adv. Mater.*, 2018, **30**, 1706330.
41 R. R. Liang, S. Q. Xu, L. Zhang, R. H. A, P. Chen, F. Z. Cui, Q. Y. Qi, J. Sun and X. Zhao, *Nat. Commun.*, 2019, **10**, 4609.
42 R. Kamai, K. Kamiya, K. Hashimoto and S. Nakanishi, *Angew. Chem., Int. Ed.*, 2016, **55**, 13184–13188.
43 I. Hijazi, T. Bourgeteau, R. Cornut, A. Morozan, A. Filoramo, J. Leroy, V. Derycke, B. Jousselme and S. Campidelli, *J. Am. Chem. Soc.*, 2014, **136**, 6348–6354.
44 H. Jia, Z. Sun, D. Jiang and P. Du, *Chem. Mater.*, 2015, **27**, 4586–4593.
45 C. S. Diercks and O. M. Yaghi, *Science*, 2017, **355**, eaal1585.
46 K.-H. Wu, D.-W. Wang, D.-S. Su and I. R. Gentle, *ChemSusChem*, 2015, **8**, 2772–2788.
47 H. B. Yang, J. Miao, S.-F. Hung, J. Chen, H. B. Tao, X. Wang, L. Zhang, R. Chen, J. Gao, H. M. Chen, L. Dai and B. Liu, *Sci. Adv.*, 2016, **2**, e1501122.
48 H. V. Babu, M. G. M. Bai and M. R. Rao, *ACS Appl. Mater. Interfaces*, 2019, **11**, 11029–11060.



 

49 X. Cui, Y. Chen, M. Zhang, Y. W. Harn, J. Qi, L. Gao, Z. L. Wang, J. Huang, Y. Yang and Z. Lin, *Energy Environ. Sci.*, 2020, **13**, 1743–1752.
50 X. Zhao, P. Pachfule and A. Thomas, *Chem. Soc. Rev.*, 2021, **50**, 6871–6913.
51 Z. Meng, R. M. Stolz and K. A. Mirica, *J. Am. Chem. Soc.*, 2019, **141**, 11929–11937.
52 H. Li, J. Chang, S. Li, X. Guan, D. Li, C. Li, L. Tang, M. Xue, Y. Yan, V. Valtchev, S. Qiu and Q. Fang, *J. Am. Chem. Soc.*, 2019, **141**, 13324–13329.
53 R. Gutzler and D. F. Perepichka, *J. Am. Chem. Soc.*, 2013, **135**, 16585–16594.
54 X. Huang, C. Sun and X. Feng, *Sci. China: Chem.*, 2020, **63**, 1367–1390.
55 S. Kandambeth, A. Mallick, B. Lukose, M. V. Mane, T. Heine and R. Banerjee, *J. Am. Chem. Soc.*, 2012, **134**, 19524–19527.
56 A. Halder, M. Ghosh, M. A. Khayum, S. Bera, M. Addicoat, H. S. Sasmal, S. Karak, S. Kurungot and R. Banerjee, *J. Am. Chem. Soc.*, 2018, **140**, 10941–10945.
57 F. Haase and B. V. Lotsch, *Chem. Soc. Rev.*, 2020, **49**, 8469–8500.
58 C. Tang, H.-F. Wang and Q. Zhang, *Acc. Chem. Res.*, 2018, **51**, 881–889.
59 J. Wang, H. Kong, J. Zhang, Y. Hao, Z. Shao and F. Ciucci, *Prog. Mater. Sci.*, 2021, **116**, 100717.
60 T. Asefa, *Acc. Chem. Res.*, 2016, **49**, 1873–1883.
61 K. Iwase, S. Nakanishi, M. Miyayama and K. Kamiya, *ACS Appl. Energy Mater.*, 2020, **3**, 1644–1652.
62 S. Yang, Y. Yu, M. Dou, Z. Zhang, L. Dai and F. Wang, *Angew. Chem., Int. Ed.*, 2019, **58**, 14724–14730.
63 G. Zhang, Y. Ji, C. Zhang, X. Xiong, K. Sun, R. Chen, W. Chen, Y. Kuang, L. Zheng, H. Tang, W. Liu, J. Liu, X. Sun, W.-F. Lin and H. Dai, *Energy Environ. Sci.*, 2019, **12**, 1317–1325.
64 D.-G. Wang, T. Qiu, W. Guo, Z. Liang, H. Tabassum, D. Xia and R. Zou, *Energy Environ. Sci.*, 2021, **14**, 688–728.
65 K. Yuan, D. Lutzenkirchen-Hecht, L. Li, L. Shuai, Y. Li, R. Cao, M. Qiu, X. Zhuang, M. K. H. Leung, Y. Chen and U. Scherf, *J. Am. Chem. Soc.*, 2020, **142**, 2404–2412.
66 Y. Chen, S. Ji, Y. Wang, J. Dong, W. Chen, Z. Li, R. Shen, L. Zheng, Z. Zhuang, D. Wang and Y. Li, *Angew. Chem., Int. Ed.*, 2017, **56**, 6937–6941.
67 L. Li, Y. Li, Y. Xiao, R. Zeng, X. Tang, W. Yang, J. Huang, K. Yuan and Y. Chen, *Chem. Commun.*, 2019, **55**, 7538–7541.
68 S. Chen, L. Zhao, J. Ma, Y. Wang, L. Dai and J. Zhang, *Nano Energy*, 2019, **60**, 536–544.
69 J. Zhang, Y. Zhao, C. Chen, Y. C. Huang, C. L. Dong, C. J. Chen, R. S. Liu, C. Wang, K. Yan, Y. Li and G. Wang, *J. Am. Chem. Soc.*, 2019, **141**, 20118–20126.
70 Y. Li, Z. Zhou, P. Shen and Z. Chen, *ACS Nano*, 2009, **3**, 1952–1958.
71 A. Ambrosi, C. K. Chua, N. M. Latiff, A. H. Loo, C. H. A. Wong, A. Y. S. Eng, A. Bonanni and M. Pumera, *Chem. Soc. Rev.*, 2016, **45**, 2458–2493.
72 E. Cruz-Silva, F. Lopez-Urias, E. Munoz-Sandoval, B. G. Sumpter, H. Terrones, J.-C. Charlier, V. Meunier and M. Terrones, *ACS Nano*, 2009, **3**, 1913–1921.
73 W. Lei, Y.-P. Deng, G. Li, Z. P. Cano, X. Wang, D. Luo, Y. Liu, D. Wang and Z. Chen, *ACS Catal.*, 2018, **8**, 2464–2472.
74 X. Zhang, Z. Lu, Z. Fu, Y. Tang, D. Ma and Z. Yang, *J. Power Sources*, 2015, **276**, 222–229.
75 I.-Y. Jeon, S. Zhang, L. Zhang, H.-J. Choi, J.-M. Seo, Z. Xia, L. Dai and J.-B. Baek, *Adv. Mater.*, 2013, **25**, 6138–6145.
76 Z. Yang, Z. Yao, G. Li, G. Fang, H. Nie, Z. Liu, X. Zhou, X. a. Chen and S. Huang, *ACS Nano*, 2012, **6**, 205–211.
77 D. Li, C. Li, L. Zhang, H. Li, L. Zhu, D. Yang, Q. Fang, S. Qiu and X. Yao, *J. Am. Chem. Soc.*, 2020, **142**, 8104–8108.
78 X. Zhu, C. Hu, R. Amal, L. Dai and X. Lu, *Energy Environ. Sci.*, 2020, **13**, 4536–4563.
79 L. Yang, S. Jiang, Y. Zhao, L. Zhu, S. Chen, X. Wang, Q. Wu, J. Ma, Y. Ma and Z. Hu, *Angew. Chem., Int. Ed.*, 2011, **50**, 7132–7135.
80 J. Liu, Y. Hu and J. Cao, *Catal. Commun.*, 2015, **66**, 91–94.
81 S. Y. Yu, J. Mahmood, H. J. Noh, J. M. Seo, S. M. Jung, S. H. Shin, Y. K. Im, I. Y. Jeon and J. B. Baek, *Angew. Chem., Int. Ed.*, 2018, **57**, 8438–8442.
82 S. Wu, M. Li, H. Phan, D. Wang, T. S. Herng, J. Ding, Z. Lu and J. Wu, *Angew. Chem., Int. Ed.*, 2018, **57**, 8007–8011.
83 W. Li, Z. Zhao, W. Hu, Q. Cheng, L. Yang, Z. Hu, Y. A. Liu, K. Wen and H. Yang, *Chem. Mater.*, 2020, **32**, 8553–8560.
84 C. Yang, Z.-D. Yang, H. Dong, N. Sun, Y. Lu, F.-M. Zhang and G. Zhang, *ACS Energy Lett.*, 2019, **4**, 2251–2258.
85 S. Mondal, B. Mohanty, M. Nurhuda, S. Dalapati, R. Jana, M. Addicoat, A. Datta, B. K. Jena and A. Bhaumik, *ACS Catal.*, 2020, **10**, 5623–5630.
86 R. Jasinski, *Nature*, 1964, **201**, 1212–1213.
87 M. Qiao, Y. Wang, Q. Wang, G. Hu, X. Mamat, S. Zhang and S. Wang, *Angew. Chem., Int. Ed.*, 2020, **59**, 2688–2694.
88 L. Gong, H. Zhang, Y. Wang, E. Luo, K. Li, L. Gao, Y. Wang, Z. Wu, Z. Jin, J. Ge, Z. Jiang, C. Liu and W. Xing, *Angew. Chem., Int. Ed.*, 2020, **59**, 2–8.
89 Q. Yang, Y. Jia, F. Wei, L. Zhuang, D. Yang, J. Liu, X. Wang, S. Lin, P. Yuan and X. Yao, *Angew. Chem., Int. Ed.*, 2020, **59**, 6122–6127.
90 Y. Lian, W. Yang, C. Zhang, H. Sun, Z. Deng, W. Xu, L. Song, Z. Ouyang, Z. Wang, J. Guo and Y. Peng, *Angew. Chem., Int. Ed.*, 2020, **59**, 286–294.
91 H. Zhang, H. T. Chung, D. A. Cullen, S. Wagner, U. I. Kramm, K. L. More, P. Zelenay and G. Wu, *Energy Environ. Sci.*, 2019, **12**, 2548–2558.
92 L. Liu, S. Liu, L. Li, H. Qi, H. Yang, Y. Huang, Z. Wei, L. Li, J. Xu and B. Liu, *J. Mater. Chem. A*, 2020, **8**, 6190–6195.
93 L. Yang, D. Cheng, H. Xu, X. Zeng, X. Wan, J. Shui, Z. Xiang and D. Cao, *Proc. Natl. Acad. Sci. U. S. A.*, 2018, **115**, 6626–6631.
94 X. Tang, R. Cao, L. Li, B. Huang, W. Zhai, K. Yuan and Y. Chen, *J. Mater. Chem. A*, 2020, **8**, 25919–25930.
95 L. Yang, J. Shui, L. Du, Y. Shao, J. Liu, L. Dai and Z. Hu, *Adv. Mater.*, 2019, **31**, 1804799.
96 J. Y. Cheon, J. H. Kim, J. H. Kim, K. C. Goddeti, J. Y. Park and S. H. Joo, *J. Am. Chem. Soc.*, 2014, **136**, 8875–8878.
97 C. Y. Lin, L. Zhang, Z. Zhao and Z. Xia, *Adv. Mater.*, 2017, **29**, 1606635.

98 J.-D. Yi, R. Xu, Q. Wu, T. Zhang, K.-T. Zang, J. Luo, Y.-L. Liang, Y.-B. Huang and R. Cao, *ACS Energy Lett.*, 2018, **3**, 883–889.
99 H. Huang, F. Li, Y. Zhang and Y. Chen, *J. Mater. Chem. A*, 2019, **7**, 5575–5582.
100 N. Huang, K. H. Lee, Y. Yue, X. Xu, S. Irle, Q. Jiang and D. Jiang, *Angew. Chem., Int. Ed.*, 2020, **59**, 16587–16593.
101 K. Selvaraju and G. A. Babu, *Ionics*, 2019, **25**, 5939–5947.
102 A. Singh, S. Roy, C. Das, D. Samanta and T. K. Maji, *Chem. Commun.*, 2018, **54**, 4465–4468.
103 P. Peng, L. Shi, F. Huo, S. Zhang, C. Mi, Y. Cheng and Z. Xiang, *ACS Nano*, 2019, **13**, 878–884.
104 Z. Gao, L. L. Gong, X. Q. He, X. M. Su, L. H. Xiao and F. Luo, *Inorg. Chem.*, 2020, **59**, 4995–5003.
105 X. Ao, W. Zhang, Z. Li, J. G. Li, L. Soule, X. Huang, W. H. Chiang, H. M. Chen, C. Wang, M. Liu and X. C. Zeng, *ACS Nano*, 2019, **13**, 11853–11862.
106 J. Li, H. Zhang, W. Samarakoon, W. Shan, D. A. Cullen, S. Karakalos, M. Chen, D. Gu, K. L. More, G. Wang, Z. Feng, Z. Wang and G. Wu, *Angew. Chem., Int. Ed.*, 2019, **58**, 18971–18980.
107 M. Chen, C. Peng, Y. Su, X. Chen, Y. Zhang, Y. Wang, J. Peng, Q. Sun, X. Liu and W. Huang, *Angew. Chem., Int. Ed.*, 2020, **59**, 20988–20995.
108 K. Iwase, T. Yoshioka, S. Nakanishi, K. Hashimoto and K. Kamiya, *Angew. Chem., Int. Ed.*, 2015, **54**, 11068–11072.
109 H. B. Aiyappa, J. Thote, D. B. Shinde, R. Banerjee and S. Kurungot, *Chem. Mater.*, 2016, **28**, 4375–4379.
110 X. Zhao, P. Pachfule, S. Li, T. Langenhahn, M. Ye, C. Schlesiger, S. Praetz, J. Schmidt and A. Thomas, *J. Am. Chem. Soc.*, 2019, **141**, 6623–6630.
111 Z. Gao, L. L. Gong, X. Q. He, X. M. Su, L. H. Xiao and F. Luo, *Inorg. Chem.*, 2020, **59**, 4995–5003.
112 Z. Gao, Z. Yu, Y. Huang, X. He, X. Su, L. Xiao, Y. Yu, X. Huang and F. Luo, *J. Mater. Chem. A*, 2020, **8**, 5907–5912.
113 C. Liu, F. Liu, H. Li, J. Chen, J. Fei, Z. Yu, Z. Yuan, C. Wang, H. Zheng, Z. Liu, M. Xu, G. Henkelman, L. Wei and Y. Chen, *ACS Nano*, 2021, **15**, 3309–3319.
114 B.-Q. Li, S.-Y. Zhang, B. Wang, Z.-J. Xia, C. Tang and Q. Zhang, *Energy Environ. Sci.*, 2018, **11**, 1723–1729.
115 Q. Zuo, G. Cheng and W. Luo, *Dalton Trans.*, 2017, **46**, 9344–9348.

 